Chronology of Emplacement of Mesozoic Batholithic Complexes In California and Western Nevada

By J. F. EVERNDEN *and* R. W. KISTLER

GEOLOGICAL SURVEY PROFESSIONAL PAPER 623

Prepared in cooperation with the University of California (Berkeley) Department of Geological Sciences

UNITED STATES GOVERNMENT PRINTING OFFICE, WASHINGTON : 1970

UNITED STATES DEPARTMENT OF THE INTERIOR

WALTER J. HICKEL, *Secretary*

GEOLOGICAL SURVEY

William T. Pecora, *Director*

Library of Congress catalog-card No. 78-603860

For sale by the Superintendent of Documents, U.S. Government Printing Office
Washington, D.C. 20402 - Price $1.25 (paper cover)

CONTENTS

ILLUSTRATIONS

TABLES

CHRONOLOGY OF EMPLACEMENT OF MESOZOIC BATHOLITHIC COMPLEXES IN CALIFORNIA AND WESTERN NEVADA

By J. F. Evernden [1] and R. W. Kistler

ABSTRACT

Ar^{40}/K^{40} was determined for minerals from specimens of Mesozoic granitic rocks collected at 250 localities in California and western Nevada. Analytical reproducibility of Ar^{40}/K^{40} in common minerals from granitic rocks was tested in the laboratories of the U.S. Geological Survey and University of California (Berkeley), and the results were studied for interpretation of the genetic significance of potassium-argon ages derived from the ratios.

The potassium-argon ages of minerals from Mesozoic granitic rocks in California have a continuity from 210 to 80 million years ago. However, a distinct periodicity of magma generation and intrusion is shown when the ages are related to the distribution of genetic groups of plutons based on geologic mapping. Five epochs of magma generation and emplacement that took from 10 to 15 million years to complete were initiated at approximately 30-million year intervals. Each intrusive epoch was preceded by, or was in part contemporaneous with, a period of regional deformation in California or western Nevada. These intrusive epochs and their ages are:

Maximum to minimum age (m.y.)	*Geologic age*	*Intrusive epoch*
90–79	Late Cretaceous	Cathedral Range.
121–104	Early Cretaceous	Huntington Lake.
148–132	Late Jurassic	Yosemite.
180–160	Early and Middle Jurassic	Inyo Mountains.
210–195	Middle and Late Triassic	Lee Vining.

INTRODUCTION

The motivations for this study derive both from the desire to investigate and document further the influence of various factors on the precision and accuracy attainable in the measurement of potassium-argon ratios in minerals of granitic rocks and from an interest in the problem of genesis and emplacement of pluton complexes such as those of California and western Nevada. Study emphasis is on the well-exposed Sierra Nevada batholith in California.

It must be made clear that precision and accuracy as used here refer only to problems of potassium and argon measurement and not to the meaning of "apparent ages." Accepting this as the only possible meaning to be signified by plus or minus estimates on determined "ages," there is very little documentation of factors influencing such plus or minus estimates. Moreover, highly variable statements are still made by different investigators with little or no supporting data. Some investigators report ages with "probable errors of about 5 percent," while others imply precision of 1 percent. The data of the present paper clearly show the influence of diverse factors on precision and accuracy of potassium-argon ages. The investigation of determined potassium-argon ratios as a function of mineral alteration or other factors has indicated the necessity of considering such factors in the interpretation of derived "ages."

Data previously presented (Evernden and Richards, 1962) on the Paleozoic batholiths of eastern Australia strongly suggested that there had been continuity of granite generation and emplacement over a period of some 200 million years. The locus of batholithic intrusion moved more than 300 km, but the "ages" obtained implied the virtual lack of any cessation of emplacement of granitic magma during that long interval. On the other hand, previous interpretations of ages of granitic rocks from the Sierra Nevada of California have implied at least two distinct periods of granite emplacement (Curtis and others, 1958). Kistler, Bateman, and Brannock (1965) have suggested three possible age groups.

We show that the patterns of ages of granitic rocks in the Sierra Nevada, taken altogether, have a continuity similar to that of the ages of granitic rocks in eastern Australia. However, a distinct periodicity of magma generation and intrusion is shown when potassium-argon and rubidium-strontium ages are related to the distribution of genetic groups of plutons based on geologic mapping. We also show that the thermal history of individual plutons is reflected in their mineral ages and that, with a few assumptions, the data permit estimates of the crustal level of emplacement of the plutons.

An essential assumption in the discussion that follows

[1] Present affiliation, Advanced Research Projects Agency, Washington, D.C.

is that the "ages" obtained by potassium-argon analysis result primarily from a more or less complex cooling history for each pluton and mineral. Virtually all investigators have concluded that the plutons of the Sierra Nevada are the product of magmatic emplacement. In fact, the pattern of ages obtained seems to be inconsistent with any other interpretation. Assuming this and assuming no later reheating of the rock, then at best the potassium-argon age of a mineral from the rock will be a determination of the time when this magma mass had cooled sufficiently to allow retention of argon in the crystal lattice. Because of pronounced difference in diffusion rate in relation to temperature for argon in biotite and hornblende (Hart, 1964), the amount of discordance between biotite and hornblende ages from rocks will be, in some sense, a measure of the cooling rate of the pluton. Thus, concordance of these two ages implies rapid cooling and a near approach of the determined age to the time of initiation of cooling of the pluton. On the other hand, reheating of the sample by later intrusion will result in partial or complete loss of previously generated argon and will often give rise to marked discordance in biotite and hornblende ages. If the pattern of discordance is accurately delineated, conclusions about the pattern of growth of the pluton complexes become possible.

Many of the samples collected for this study are from areas that are virtually unmapped in terms of delineation of individual plutons. This is unfortunate, but we point out that the great span of time, Late Triassic to Late Cretaceous, represented by the Mesozoic intrusive rocks of California, is demonstrated mainly by the data of geochronometry and not by stratigraphic correlation. In fact, even in areas of detailed mapping, the ages of intruded rocks are so poorly known, or stratigraphic columns have such large gaps, that geologic assignment of ages of intrusive rocks is usually possible only within the limits of two or more geologic periods. It was decided, therefore, that questions of sufficient interest for this study could be answered without further detailed field control, while such a pattern of dates as here demonstrated may act as a stimulus to field investigations.

Prior to the writing of the paper, we had been dating rocks independently in different areas of the Sierra Nevada and adjacent batholiths of California and western Nevada as part of work at the University of California (Berkeley) and the Geological Survey. In order to present as comprehensive a report as is possible at present and to facilitate the publication of the large mass of data gathered, we combined our efforts for this paper.

The discussions separate logically into two parts. The first part deals with analytical problems such as the precision and accuracy of potassium measurements (a similar treatment for argon measurements is to be found in Evernden and Curtis, 1965) and the influence of chemical and mineralogic factors on apparent potassium-argon ages. The second part is the geologic interpretation of the total body of the absolute age data. The two parts can be read as nearly separate papers.

ANALYTICAL PROBLEMS

ANALYTICAL PROCEDURES

Standard analytical techniques for potassium and argon used at the University of California (Berkeley) are described in Evernden and Curtis (1965); similar techniques used by the U.S. Geological Survey are described in Kistler and Dodge (1966). Precision and accuracy obtained for potassium-argon ages at UC Berkeley have been reported by Evernden, Savage, Curtis, and James (1964); those obtained by the Geological Survey by Kistler (1968).

The rubidium-strontium analyses of granitic rocks that are reported in this paper were made by Carl Hedge or by Kistler. Rubidium and strontium were determined by standard isotope dilution techniques and by X-ray fluorescence analyses.

Localities of all analyzed specimens are shown on plate 1 and are tabulated in table 5 of this report. Potassium-argon ages of biotite and (or) hornblende are shown for each locality on plate 2. Potassium-argon analytical data are tabulated in table 5 and rubidium-strontium analytical data are tabulated in table 4. Rock names and descriptions are given in table 6.

PRECISION AND ACCURACY

POTASSIUM DETERMINATIONS

All potassium analyses at UC Berkeley were made by means of a flame photometer with a propane flame. The galvanometer was replaced by one having greater precision of movement. NH_4OH and $(NH_4)_2CO_3$ are made in the laboratory; all other chemicals are reagent grade. All measurements are made against carefully buffered standards; all new determinations are made in duplicate; and with every set of four new determinations, a repeat of a previously analyzed specimen is performed. Blank runs now yield values between 0.013 and 0.018 ppm potassium in 200-cc solution.

The problem to be approached first is that of reproducibility of results by the technique used. The first requirement of such an evaluation is the use of a concentrate of very high purity. As will be demonstrated below, this is not easily obtained. However, one such concentrate of leucite has been available in large quantity and 31 analyses on it were run during 33 months. The average potassium value was 15.793 percent with the standard deviation of a single determination equal to 0.020, or the coefficient of variation of a single determination equal to 0.13 percent. These calculations were based upon normal distribution theory, but no single determination departed from the mean by more than 0.25 (twice the coefficient of variation). Another sample, NBS 99, was run 21 times during the same period of time with a mean potassium value of 0.331 percent; the standard deviation of a single determination was 0.002 percent, and the coefficient of variation was 0.6 percent (samples dried at 105°C for 24 hours). Neither of these series showed an observable drift of determined potassium value with time, although the standard solutions have been stored in polyethylene bottles with screw tops. Other shorter series also support the conclusion that, on materials of high purity or uniformity containing several percent potassium, the coefficient of variation of a laboratory's precision should be a small fraction of 1 percent, and at the 90-percent confidence level, below 1 percent.

To achieve as high purity in the biotite concentrates as was consistent with reasonable expense, samples were handpicked under a binocular microscope in the size ranges 10/16 and 16/28 Tyler mesh (exceptions to these size ranges are noted in table 5). All samples were run in duplicate. For statistical purposes, if all biotite samples were considered equal in regard to variability within the concentrates, then all samples should have the same coefficient of variation. We can treat the data as two independent sets of determinations, Set 1 (x) being the first value for each of the 141 samples, and Set 2 (y) the second value. The complete independence of Set 1 and Set 2 allows us to write

$$\sigma'^2_{(x-y)} = \sigma'^2_x + \sigma'^2_y = 2\sigma'^2_x.$$

Observed values of $(x-y)$ yield $\sigma'^2_{(x-y)} = 0.1752$ percent or $\sigma'_x = 0.296$ percent and $\sigma'_{(x+y)/2} = 0.210$ percent (all σ' values being coefficients of variation).

Thus the coefficient of variation of the mean of the two determined values is, according to normal distribution theory as applied to all of the data, two-tenths of 1 percent, and the coefficient of variation of a single determination is 0.3 percent. Two points should be noted: the σ_x' value is higher than would be expected from a consideration of the leucite data, and the $(x-y)$ values do not show a normal distribution (fig. 1). These facts suggest that the pattern of figure 1 is not controlled solely by laboratory reproducibility but that additional factors are influencing the distribution. Chlorite content of the biotite grains seems to be the explanation. We have previously noted that it is impossible to obtain uniform splits of nonuniform samples. Many of the samples concentrated are from rock which, in thin section, appeared practically useless because of extensive chloritization. However, by crushing a few pounds of rock and by carefully picking grains which displayed no obvious chlorite content under reflected light, samples with potassium values above 7 percent were obtained in most cases. Biotite

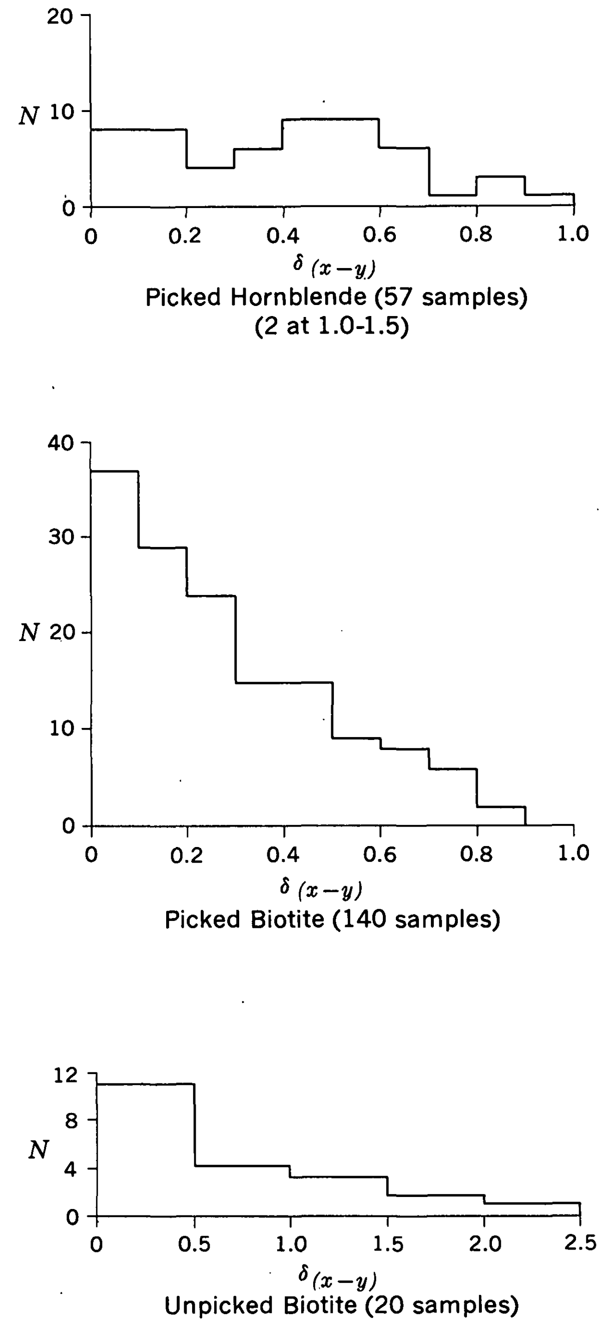

FIGURE 1.—Histograms of $\delta_{(x-y)}$ values. N is number of samples.

books from such rocks often contain appreciable chlorite detectable only by further disaggregation of the books. Three lines of evidence suggest that this chlorite content is the explanation of the high σ' computed. Firstly, the observed $(x-y)$ values are a function of potassium content of the biotite; the mean of all samples with $\delta_{(x-y)}$ less than 0.1 percent is 7.6 percent potassium, whereas the mean of all samples with $\delta_{(x-y)}$ greater than 0.5 percent is 7.3 percent potassium ($\delta_{(x-y)}$ being $(x-y)$ expressed as percent of the potassium value). Secondly, the $\delta_{(x-y)}$ values are a function of the sample and are not randomly distributed throughout the set of determinations. The evidence for this was obtained by repeated potassium analyses. Four samples with $\delta_{(x-y)}$ less than 0.1 percent and four with $\delta_{(x-y)}$ greater than 0.5 percent were rerun in duplicate; the second $\delta_{(x-y)}$ values are here termed $\delta_{(x-y)}{}^{n}$.

	$\delta_{(x-y)}$ (percent)	$\delta_{(x-y)n}$ (percent)
KA 1540	0. 03	0. 1
1568	. 05	. 09
1573	. 1	. 01
1575	. 04	. 09
1525	. 7	. 6
1537	. 8	. 5
1591	. 8	. 8
1593	. 9	. 6

Thirdly, several samples with $\delta_{(x-y)}$ values below 0.1 percent and above 0.5 percent were crushed and examined under the petrographic microscope. Invariably, those with high values of $\delta_{(x-y)}$ showed appreciable chlorite, whereas those with low values of $\delta_{(x-y)}$ showed little or no chlorite. A further demonstration of this correlation of high $\delta_{(x-y)}$ values with low potassium content and thus with appreciable chlorite and resulting inhomogeneity of sample is obtainable by comparing the potassium and $\delta_{(x-y)}$ values of picked and unpicked (P and U) samples in table 5 (all $\delta_{(x-y)}$ values are there rounded to the closest tenth percent) and by inspection of figure 1. It appears that the correlation of $\delta_{(x-y)}$ values and chlorite content is established and that such chlorite content degrades the precision or accuracy obtainable. We suggest, therefore, that all reported potassium-argon ages should include as an essential piece of information the $\delta_{(x-y)}$ values for each age determination, assuming that duplicate potassium analyses are performed. Note that virtually all the hornblendes have $\delta_{(x-y)}$ values of several tenths of 1 percent or higher (fig. 1), indicating a lower precision and accuracy for these "ages" than for the biotite ages.

Interlaboratory comparisons based upon samples showing high values of $\delta_{(x-y)}$ are pointless because it becomes difficult or impossible to separate laboratory differences from sample variation.

The main geologic conclusions of this paper will be based upon a study of the relative ages of both biotite and hornblende obtained for the numerous samples. As all the biotites and hornblendes are similar chemically there is no reason to expect that the results of flame-photometry procedures have significant errors in relative values greater than those of the analytical precision discussed above. Errors in analysis by flame photometry are of a systematic character, not random. Crosschecks against other laboratories and against results from different analytical techniques yield estimates of the accuracy of the determined potassium values, and thus of the accuracy obtainable with the procedures used. The following data have been recently obtained in a continuing effort to evaluate accuracy:

1. UC Berkeley values (Evernden and Curtis, 1965) on biotite B 3203, 7.54, 7.57, 7.58, and 7.56 percent K, which are in good agreement with other published values (for example, see Hart, 1964, who reports a K value of 7.56 percent).
2. Results on samples run at both the University of California (Berkeley) and the Geological Survey by flame photometer but using different preparation procedures, and results of Survey analysis of actinolite and aegerine augite by atomic absorption (see unnumbered table).

Flame photometer results on samples run at both University of California (Berkeley) and the U.S. Geological Survey

Sample	Atomic absorption (percent)	K (USGS) Flame photometer (percent; all values represent average of two determinations)		K (UC Berkeley) Flame photometer (percent)
B 53–15A (actinolite).	0. 060	0. 060	0. 0626	(0. 0639, 0. 0634, 0. 0609, 0. 0621)
FD–13 (plagioclase)		. 267	. 272	(0. 271, 0. 272)
CL–1 (plagioclase)		. 329	. 324	(0. 3205, 0. 3279)
422–H (aegerine augite)	0. 54	. 054	0. 54	(0. 0534, 0. 0546, 0. 0536, 0. 0543)
KA 1508–B (biotite)		7. 51	7. 55	(7. 53, 7. 57)
KA 1566–B (biotite)		7. 36	7. 55	(7. 53, 7. 57)
FD–13 (biotite)		7. 75	7. 86	(7. 85, 7. 86)

3. Feldspars analyzed at UC Berkeley by two techniques: flame photometry (by J. Hampel) and X-ray fluorescence (by R. Jack); results are tabulated and shown in percent (see unnumbered table). A comparison of columns 5 and 6 of the table suggests a correlation, as the mean ϵ' for

$\delta_{(x-y)}$ less than 0.5 is 0.32, whereas the mean ϵ' for $\delta_{(x-y)}$ equal to or greater than 0.5 is 1.27. This agrees with the conclusion drawn from the biotite data; that is, large $\delta_{(x-y)}$ values are associated with nonuniform samples.

Feldspar analyses made by University of California (Berkeley)

Sample	1 K (F/P)	2 K (X/R)[G-1]	3 ϵ	4 K (X/R)[ADJ]	5 ϵ'	6 $\delta_{(x-y)}$
KA 1040	2. 562	2. 546	0. 62	2. 558	0. 15	0. 2
1044	2. 569	2. 554	. 58	2. 566	. 10	. 2
1053	3. 237	3. 225	. 37	3. 243	−. 18	. 4
1041	3. 245	3. 266	−. 34	3. 274	−. 89	. 6
1029	3. 949	3. 893	1. 42	3. 917	. 82	. 6
1051	4. 203	4. 164	. 93	4. 190	. 32	. 8
1017	4. 724	4. 630 4. 646	1. 82	4. 669	1. 16	. 6
1090	4. 962	5. 048	−1. 73	5. 081	−2. 40	. 6
1178	5. 253	5. 250	. 06	5. 286	. 63	. 2
1089	5. 290	5. 249	. 78	5. 286	. 08	. 2
1054	5. 307	5. 363	−1. 06	5. 400	−1. 76	. 7
1193	5. 390	5. 391	. 02	5. 354	. 67	. 4
1365	5. 798	5. 731	1. 16	5. 774	. 42	. 2
G-1	4. 600	"4. 499"	2. 2	4. 529	1. 55	. 5

1. Potassium values obtained by flame photometry.
2. Potassium values obtained by X-ray fluorescence, assuming a K value of 4.499 percent for G-1.
3. (Column 1 − Column 2)×100/Column 1.
4. Potassium values obtained by X-ray fluorescence, calibration being controlled by plot of Column 1 versus Column 2 and adjustment indicated.
5. (Column 1 − Column 4)×100/Column 1.
6. Difference between the two K values obtained by flame photometry, expressed as percent of K value.

4. Potassium analyses repeated after 6 years on unpicked biotite samples. New runs have numbers ending in (−64):

Run No.	KA 67	KA 67–64	KA 71	KA 71–64	KA 72	KA 72–64
K (percent)	7. 09	7. 21	7. 55	7. 52	7. 53	7. 59

Both runs were performed on flame photometers, but by somewhat different preparation procedures.

ARGON DETERMINATIONS

Argon analyses are not routinely repeated. Control on argon precision and accuracy is obtained by repeats on several selected samples and by doing large numbers of genetically or temporally related samples. Thus, when dating volcanic rocks related to strata that yielded vertebrate fossils, the accuracy of the dates and other conclusions of the investigation were substantiated by a large body of age determinations related to many sites (Evernden and others, 1964). In the present investigation, several biotite samples were run in duplicate; in other words, splits of the same mineral concentrate were used in two independent argon analyses. All samples with numbers between KA 1432 and KA 1713 were analyzed by using spikes from a single spike set; this procedure eliminates any possible relative difference of age due to failure to intercalibrate different spike sets accurately. The data on repeat runs are given in table 1 (all runs are on *picked* samples). The mean difference of the picked biotite paired runs is 0.68 percent of the age. If the anomalously high value of KA 1608 is excluded, the mean difference is 0.48 percent. We can only suggest misweighing or undetected blow-out as possible causes of the discrepancy of the KA 1608 pair.

TABLE 1.—*Potassium-argon ages of minerals with duplicate argon analyses*

Run	Mineral	K (percent)	"Age" (m.y.)	Ar^{40}_{at} (percent)
KA 1508	Biotite	7. 821	86. 8	7
1508–R			86. 6	8
1508–B	Biotite; second concentrate.	7. 549	88. 9	6
1508–B–R			89. 0	7
1518	Biotite	7. 571	87. 1	14
1518–R			87. 4	15
1526	Biotite	7. 778	82. 4	8
1526–R			83. 7	7
1538	Biotite	7. 591	83. 0	5
1538–R			83. 6	8
1541	Biotite	7. 705	94. 4	6
1541–R			94. 0	7
1548	Biotite	6. 994	81. 5	9
1548–R			81. 8	6
1566	Biotite	7. 618	87. 8	9
1566–R			88. 2	10
1566–B	Biotite; second concentrate.	7. 548	88. 7	9
1566–B–R			88. 2	10
1587	Biotite	7. 623	78. 4	4
1587–R			78. 4	10
1590	Biotite	7. 391	81. 9	11
1590–R			81. 5	16
1608	Biotite	7. 099	90. 5	15
1608–R			93. 2	10
1442	Hornblende; 28/48 Tyler mesh.	. 4515	143	32
1449	Hornblende; 35/48 Tyler mesh.	. 4512	142	14
67	Biotite	7. 09	91. 0	13
67–64	Biotite; same concentrate, rerun, 6 years later, unpicked.	7. 21	93. 3	9
71	Biotite	7. 55	88. 5	7
71–64	Biotite; same concentrate, rerun, 6 years later, unpicked.	7. 516	92. 9	9
72	Biotite	7. 59	87. 8	17
72–64	Biotite; same concentrate, rerun, 6 years later, unpicked.	7. 531	90. 0	11

By duplicate analysis of argon from biotite, sanidine, and plagioclase from four USGS samples, the mean difference of paired runs is 1.3 percent of the age (Kistler, 1968).

A cross check between UC Berkeley and the Geological Survey served to intercalibrate the data from the two laboratories:

FD-13 Biotite	UC Berkeley	124.9×10^{-11} moles/gram Ar^{40}_{Rad}
	USGS	126.0×10^{-11} moles/gram Ar^{40}_{Rad}

The UC Berkeley value represents a single determination, the USGS value the average of two analyses (125.3, 126.8).

CHEMICAL AND CRYSTALLOGRAPHIC EFFECTS ON POTASSIUM-ARGON AGES

APPARENT AGE AS A FUNCTION OF CHLORITE CONTENT OF BIOTITE

The discussion so far has been concerned solely with the reproducibility of potassium and argon analyses of given mineral concentrates. A matter of real concern is the effect of grain size and (or) chemical composition on the apparent age of a mineral concentrate. (See the following section, "Apparent age as a function of mineral type," for discussion of comparisons of apparent ages obtained from different minerals of the same rock sample, specifically for the minerals biotite, hornblende, potassium feldspar, plagioclase, and quartz.) The influence of chlorite content on age was investigated by analysis of two biotite-samples, one only slightly chloritized (KA 1511), the other extensively chloritized (KA 1527). The results are shown in table 2.

TABLE 2.—*Data showing variation of potassium-argon age with variation in chlorite content in biotite*

Run	Picked (P) or unpicked (U)	Size (Tyler)	K (percent)	Age (m.y.)	$(x-y)$ (percent)
Few percent chlorite content in biotite books					
KA 1511	P	16/28	7. 438	97. 2	0. 1
1511–10/16	U	10/16	6. 699	97. 5	. 7
1511–16/28	U	16/28	6. 176	98. 5	. 1
1511–35/48	U	35/48	6. 799	101. 4	. 7
1511–100/150	U	100/150	7. 093	100. 9	. 1
1511–HBD	P	35/60	. 876	124. 6	. 5
Very high chlorite content in biotite					
KA 1527	P	10/16	7. 602	81. 9	0. 0
1527–8/10	U	8/10	7. 315	80. 2	. 8
1527–10/16	U	10/16	7. 166	80. 0	. 4
1527–16/28	U	16/28	6. 880	82. 0	. 3
1527–35/48	U	35/48	4. 344	85. 7	. 1
1527–48/60	U	48/60	3. 171	86. 9	1. 5
1527–60/100	U	60/100	2. 825	84. 7	. 1
1527–100/150	U	100/150	1. 630	90. 8	. 6
1533–HBD	P	28/60	. 670	84. 3	. 0

Unpicked means that the biotite-chlorite concentrate was obtained by sizing and by using heavy liquids and that all other easily identified grains were removed by picking, care being taken not to alter the biotite-chlorite in the concentrate. Therefore, the slight increase of apparent age with decreasing grain size in KA 1511 cannot with certainty be separated from the possible presence of hornblende, although a 13 percent hornblende content would be required to explain the indicated increase in age in KA 1511–100/150. Note that the hornblende in this rock (table 2, KA 1511–HBD) is older than the biotite. The selection of this biotite for size analysis was made on the basis of its low content of chlorite prior to discovering the discordant biotite-hornblende ages. These data are still in marked contrast to those from KA 1527. In the KA 1527 series, the concentration of chlorite in the small grain sizes is clearly shown by the four- to five-fold decrease in potassium content with decreasing grain size. The apparent ages, though not rising in a perfectly systematic manner, increase by over 10 percent with the decrease of potassium. Run KA 1533–HBD, done on a hornblende sample taken from the same end of the same pluton as KA 1527 (Cathedral Peak pluton, see fig. 2), indicates that the increase in apparent age in the KA 1527 series cannot be attributed to the included hornblende. Numerous samples from the south end of the Cathedral Peak pluton (fig. 2) have been analyzed with the apparent ages showing a seeming correlation with potassium content (all samples picked):

Run	Size (Tyler mesh)	K (percent)	Age (m.y.)	Elevation (ft)
KA 1527	10/16	7. 602	81. 9	8, 800
1533	16/28	7. 545	82. 5	8, 800
1531	16/28	7. 443	83. 6	9, 000
1594	16/28	7. 120	82. 4	8, 700
1593	16/28	7. 100	83. 4	10, 900
1530	10/16	7. 053	83. 7	9, 000
1528	16/28	6. 845	84. 6	8, 800

Five samples from the north end of the same pluton show the following relationship:

Run	Size (Tyler mesh)	K (percent)	Age (m.y.)	Elevation (ft)
KA 1598	16/28	7. 598	80. 1	7, 300
1597	16/28	7. 435	80. 2	7, 950
1595	16/28	7. 296	81. 0	11, 000
1599	16/28	7. 208	81. 4	9, 000
1596	28/48	6. 979	81. 4	9, 200

The set from the north end may not be significant, but the set from the south end is certainly significant in light of the initial discussion of reproducibility of potassium and argon values. The suite of samples from the southern end of the pluton shows a strong correlation of potassium content and apparent age, as does the sequence of sized samples of KA 1527, a member of the suite. The explanation is not at all obvious. As a matter of fact, the correlation is exactly opposite to that expected. Much of the chloritization in these rocks is a weathering phenomenon rather than the result of deuteric processes. Furthermore, it would seem quite impossible to explain the above data in terms of chlorite development at time of emplacement. The only possible explanation must be in terms of a weathering process which achieved more complete removal of potassium than argon during chloritization. This conclusion, in turn, would seem consistent only with many of the argon atoms being in nonpotassium (octahedral layer?) lattice sites, that is, sites less subject to destruction during chloritization. Thus, we may have obtained definitive evidence that many argon atoms are impelled into nonpotassium lattice sites by recoil at time of disintegration of the potassium and associated gamma-ray radiation. Whatever the explanation, the obvious conclusion is that an inverse correlation of apparent age and potassium content in biotites can occur. Previously published results (Evernden and others, 1964, p. 160) are not in disagreement with this conclusion, as the potassium values for the series reported there changed by only 30 percent.

APPARENT AGE AS A FUNCTION OF MINERAL TYPE

In our haste to find answers to the more exotic problems of geochronology, many of the important details of argon distribution and retention in various minerals were not carefully investigated and are only slowly being supplied. Thus, the early rejection of all feldspars for potassium-argon analysis has been shown to have been too wide-ranging in scope. Virtually all volcanic feldspars seem to be satisfactory for potassium-argon dating throughout the Phanerozoic (Evernden and James, 1964). After the data were studied and this conclusion reached, it was not understandable why all feldspars of granitic rocks should be poor argon traps. Inspection of thin sections, however, shows that extensive alteration of both potassium-feldspar and plagioclase is virtually universal in the granitic rocks of the Sierra Nevada, and these minerals would be expected to be sources of poor potassium-argon dates. It appeared possible that use of altered or exsolved feldspars led to the early conclusions. Six relatively unaltered rocks were selected for complete analysis (table 3).

All feldspar concentrates were leached in hydrofluoric acid (Evernden and Curtis, 1965), sonically cleaned, and resized.

Four of the potassium-feldspar samples show either no microcline or only its incipient development, the potassium-argon ages of these samples being essentially concordant with the biotite ages on the same rocks (KA 1512, 1564, 1569, and 1605). Another potassium-argon age for untwinned potassium-feldspar from a Sierran granitic rock concordant with that for biotite and hornblende from the same specimen is reported in Kistler and Dodge (1966). The two potassium-feldspar samples which yielded ages in marked discordance with the biotite ages from the same rocks (KA 1533 and 1541) are extensively or completely converted to microcline.

The correlation of observed plagioclase characteristics with apparent age is not so obvious, but the six dates suggest the correlation of high argon retentivity with coarse to intermediate twinning thickness, and the correlation of low argon retentivity with alteration, thin twinning, and obvious strain. Since myrmekite is always a peripheral development, it may be that leaching with HF and sonic cleaning tend to remove such material from our concentrates, thus preventing the expected correlation of myrmekite development and deficient apparent ages.

The sample used is small, but it strongly suggests that a correlation exists between demonstrable crystal characteristics and apparent potassium-argon ages in the feldspars of instrusive rocks, a to-be-expected but as yet unsubstantiated result. The basic requirement seems to be an unrecrystallized homogeneous crystal phase with dimensions of at least several microns, that is, exactly what the study of argon retention in volcanic feldspars had indicated (Evernden and James, 1964).

APPARENT POTASSIUM-ARGON AGES OF QUARTZ FROM GRANITIC ROCKS

As first noted by Hart (1964), and as subsequently found by several investigators, it is possible to have excess quantities of argon in some pyroxenes of rocks of deep-seated origin. Exactly what "deep-seated" means in this connection is uncertain. Investigations of pyroxenes, sanidines, and plagioclases (oligoclase to bytownite) of extrusive volcanic rocks have found no argon excess. Where do granitic intrusive rocks lie in this proposed hierarchy of depth; that is, will the low-potassium minerals of granitic rocks show an argon excess? Analyzed pyroxenes of granite samples from the Sierra Nevada show the absence of excess argon (Kistler and Dodge, 1966). The sole remaining mineral present in appreciable quantity is quartz. The very low potassium content, its very late crystallization, and the possibility of gaseous inclusions within it would suggest that, if excess argon is to be found in granitic rocks, it will be found in quartz. Five quartz samples from Sierran granitic rocks have been analyzed.

Analysis of fine quartz samples from Sierran granitic rocks

Run	Mineral	K (percent)	Apparent age (m.y.)
KA 1512	Biotite	7. 429	96. 7
1512–QTZ	Quartz	. 0279	109. 4
1533	Biotite	7. 545	82. 5
1533–QTZ	Quartz	. 0250	88. 9
1541	Biotite	7. 705	94. 2
1541–QTZ	Quartz	. 0188	108. 3
1564	Biotite	7. 528	88. 5
1564–QTZ	Quartz	. 0144	57. 9
1569	Biotite	7. 971	102. 3
1569–QTZ	Quartz	. 0401	58. 1

The potassium values were obtained by flame-photometry analysis, the only technique immediately available, and it is felt that the values computed are adequate for investigating the presence of excess argon in these samples.

Sample preparation was by crushing, sizing, and heavy liquids, followed by a very strong HF leach; the intent of this leaching was to destroy all plagioclase or to so grossly alter it that it could be easily separated from the quartz by picking. The picked concentrate was again leached in HF and sonically cleaned. The quartz was fused in our standard argon-extraction lines according to the procedure outlined previously for use with very young samples (Evernden and Curtis, 1965). Pyrex bottles with vicor liners were cooled by a strong stream of air. The residue was a somewhat vesicular mass in the bottom of the molybdenum crucible, approximately half of the quartz having been vaporized and thus re-

TABLE 3—*Multimineral analyses (of same rock)*

Run	Mineral	K (percent)	Age (m.y.)	$\delta_{(x-y)}$ (percent)	Remarks based upon examination of thin section of rock
			KA 1512		
KA 1512	Biotite	7.429	96.7	0.4	Extensively chloritized (carefully picked concentrates used for analysis).
1512–HBD	Hornblende	.666	97.8	.5	Extensively chloritized (carefully picked concentrates used for analysis).
1512–PL	Plagioclase	.297	92.5	.1	Twinning thin and close. Alteration throughout grains. Virtually no myrmekite. Wavy extinction function of zoning.
1512–KF	Orthoclase	11.54	100.1	.1	Incipient microcline and very low wavy extinction.
			KA 1533		
KA 1533	Biotite	7.545	82.5	0.4	Low chlorite.
1533–HBD	Hornblende	.670	84.3	.0	Low chlorite.
1533–PL	Plagioclase	.310	70.3	3.0	Exceedingly fine twinning in some grains. Extensive alteration in coarse grains. Extensive myrmekite.
1533–KF	Orthoclase	11.95	73.5	.5	Microcline.
			KA 1541		
KA 1541	Biotite	7.705	94.4	0.7	Very low chlorite.
1541–HBD	Hornblende	.736	97.8	.9	Very low chlorite.
1541–PL	Plagioclase	.233	90.7	.1	Much myrmekite. Pronounced wavy extinction. Coarse twinning. Zoned. Less altered than KA 1533–PL.
1541–KF	Orthoclase	12.25	83.5	.5	Extensive microcline twinning. Pronounced wavy extinction.
			KA 1564		
KA 1564	Biotite	7.528	88.5	0.2	Very low chlorite.
1564–HBD	Hornblende	1.070	95.6	.9	Very low chlorite.
1564–PL	Plagioclase	.277	72.6	.8	Strong zoning. Myrmekite present but thin. Minimal wavy extinction. En echelon shear in plagioclase grains. Some distortion evident.
1564–KF	Orthoclase	11.69	87.5	.3	Essentially no microclinization. Minimum wavy extinction.
			KA 1569		
KA 1569	Biotite	7.971	102.3	0.1	Slight alteration.
1569–HBD	Hornblende	.590	107.5	.3	Slight alteration.
1569–PL	Plagioclase	.774	102.4	2.0	Big broad twins. Alteration locally strong internally and on boundaries, but not general.
1569–KF	Orthoclase	9.253	100.1	.5	Very mild strain. K-feldspar growing around plagioclase. Feathery twins locally.
			KA 1605		
KA 1605	Biotite	7.531	87.4	0.2	Slight alteration.
1605–HBD	Hornblende	.888	90.1	.2	Slight alteration.
1605–PL	Plagioclase	.254	88.7	.6	Strongly zoned. Alteration slight. Intermediate twinning density.
1605–KF	Orthoclase	11.67	87.0	--------	Incipient microclinization. Moderate wavy extinction.

moved from the crucible. There was no trouble with blowing-out of samples.

The potassium values (high for quartz) are certainly not attributable to separate grains of feldspar. They may be due to feldspar inclusions in quartz, although none were noted in thin-section examination. The distinctly higher potassium value for KA 1569–QTZ may indicate lack of removal of all altered plagioclase from the final concentrate, although the sample appeared as thoroughly fused as the others. If the data of the first four runs are averaged, the mean biotite age is 90.5 m.y. and the mean quartz age is 91.1 m.y.; the average values for all five runs are 92.8 m.y. and 84.5 m.y., respectively. The lack of any excess argon is obvious.

The environment of emplacement of the granitic rocks of the Sierra Nevada of California was such that no measurable excess argon was incorporated in any of the major minerals at time of formation, emplacement, or cooling of the plutons. Shallow emplacement, with correspondingly low confining pressure on gas content of residual fluids, is suggested by this result. Incidentally, we have found excess argon in the quartz of the Precambrian gneisses investigated by Hart (1964), in two samples of pegmatitic quartz, and in a quartz cobble from the Precambrian Witwatersrand conglomerates (unpub. data, Univ. California, Berkeley). Rama, Hart, and Roedder (1965) have reported excess argon in samples of pegmatitic and vein vuggy quartz.

GEOLOGIC INTERPRETATION

GENETIC SIGNIFICANCE OF POTASSIUM-ARGON AGES OF BIOTITE AND HORNBLENDE

POTASSIUM-ARGON AGE IN PLUTONS OF CATHEDRAL PEAK TYPE

We shall now be concerned solely with the ages obtained on biotites and on biotite-hornblende pairs. We shall assume that the patterns of ages observed have some genetic significance and shall attempt to understand the genesis of the pluton complex by a study of these ages. We shall also assume that the observed pattern of ages in these minerals is due to a complex intrusion and cooling history, that is, that argon diffusion and loss is largely a heat-dependent phenomenon. Also, we shall assume that we have largely avoided the problem of age being a function of potassium content in biotite by using carefully picked concentrates. As discussed in the first part of the report, we seem to have not completely escaped this problem in the Cathedral Peak pluton, but if this factor does not confuse the data any more than it does in that pluton, the major conclusions to be drawn from the entire body of data will be valid.

There were two main reasons for selecting plutons of Cathedral Peak type for detailed study. First, field relationships indicate they are virtually the youngest plutons of appreciable size in the Sierra Nevada. Reheating effects of later plutonism should be nonexistent, and the observed pattern of ages should reflect the pattern of emplacement and initial cooling. Secondly, plutons of this extremely distinctive rock type occur as a sequence of narrow elongate bodies along 160 miles of the Sierran crest (fig. 2, 3). The rock is a quartz monzonite typified by very large microcline phenocrysts. In several places, field mapping has not yet defined the limits of the plutons, such areas being indicated by question marks in the figures. All contacts with older rocks are essentially vertical wherever they have been clearly observed. These plutons must be considered, on the basis of field evidence, to be discrete bodies for considerable distances below the surface.

Consider first the data of the Cathedral Peak pluton. An earlier discussion showed the correlation of apparent age and potassium content. It was there shown that determined ages of carefully picked high-potassium concentrates were not strongly affected by their small chlorite content. In the present discussion, the significant points are that in carefully picked high-potassium concentrates there does not seem to be any correlation of apparent age with elevation or with east-west position but that there is a definite correlation of age with north-south position—the south end seems to be 2 to 3 m.y. older than the northern end. Since age does not seem to be a function of elevation in the pluton, an explanation of the north-south difference cannot be found in a hypothesis of pronounced tilting of the pluton. A difference due to depth of erosion is completely ruled out by field evidence. Also, if age is independent of depth, then emplacement was shallow (see below) and cooling subsequent to final emplacement was rapid; the explanation that ages are based upon the complex pattern of cooling of a pluton emplaced at all points at nearly the same time is improbable. The only hypothesis that would seem to fit the facts is one that assumes shallow emplacement and a spread of 2 to 3 m.y. in the time of final emplacement of the two ends of the pluton, that is, a history that allows final cooling of the two ends of the pluton to have been separated by 2 to 3 m.y.

The data from the Sonora pluton (fig. 2) suggest age to be a function of east-west position rather than north-south or vertical positions. In the Recess pluton (fig. 3), the few data suggest no dependence of age on north-south position, are suggestive of a correlation of age and elevation (1 m.y. per 2,000 ft), and unequivocally indicate this pluton to be younger than either of the more northerly plutons. The contrast in age between the southern end of the Cathedral Peak pluton and the northern end of the Recess pluton cannot be explained on the basis of tilt during uplift of the mountain range.

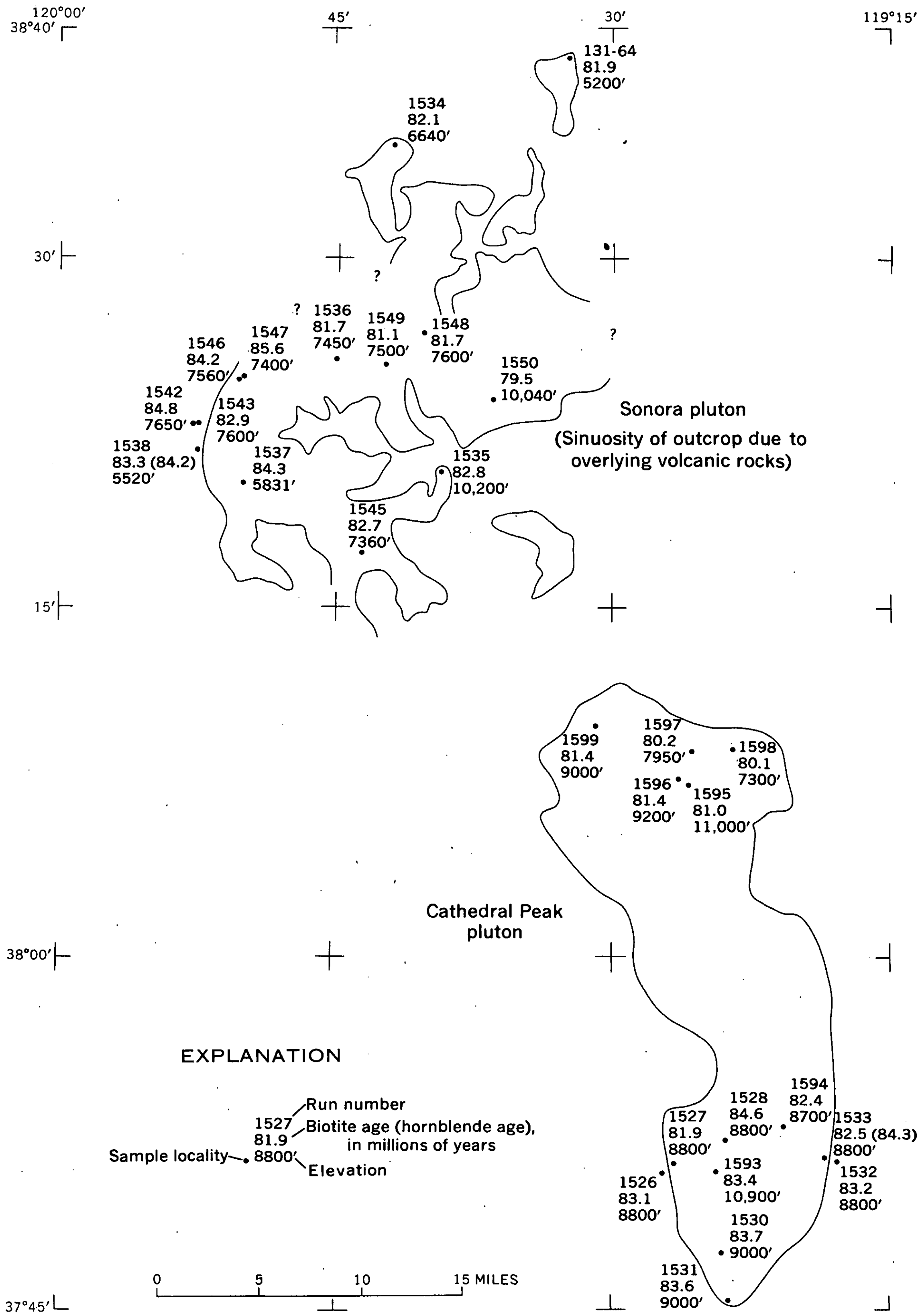

Figure 2.—Potassium-argon dates on samples from plutons of Cathedral Peak type, Sonora and Cathedral Peak plutons.

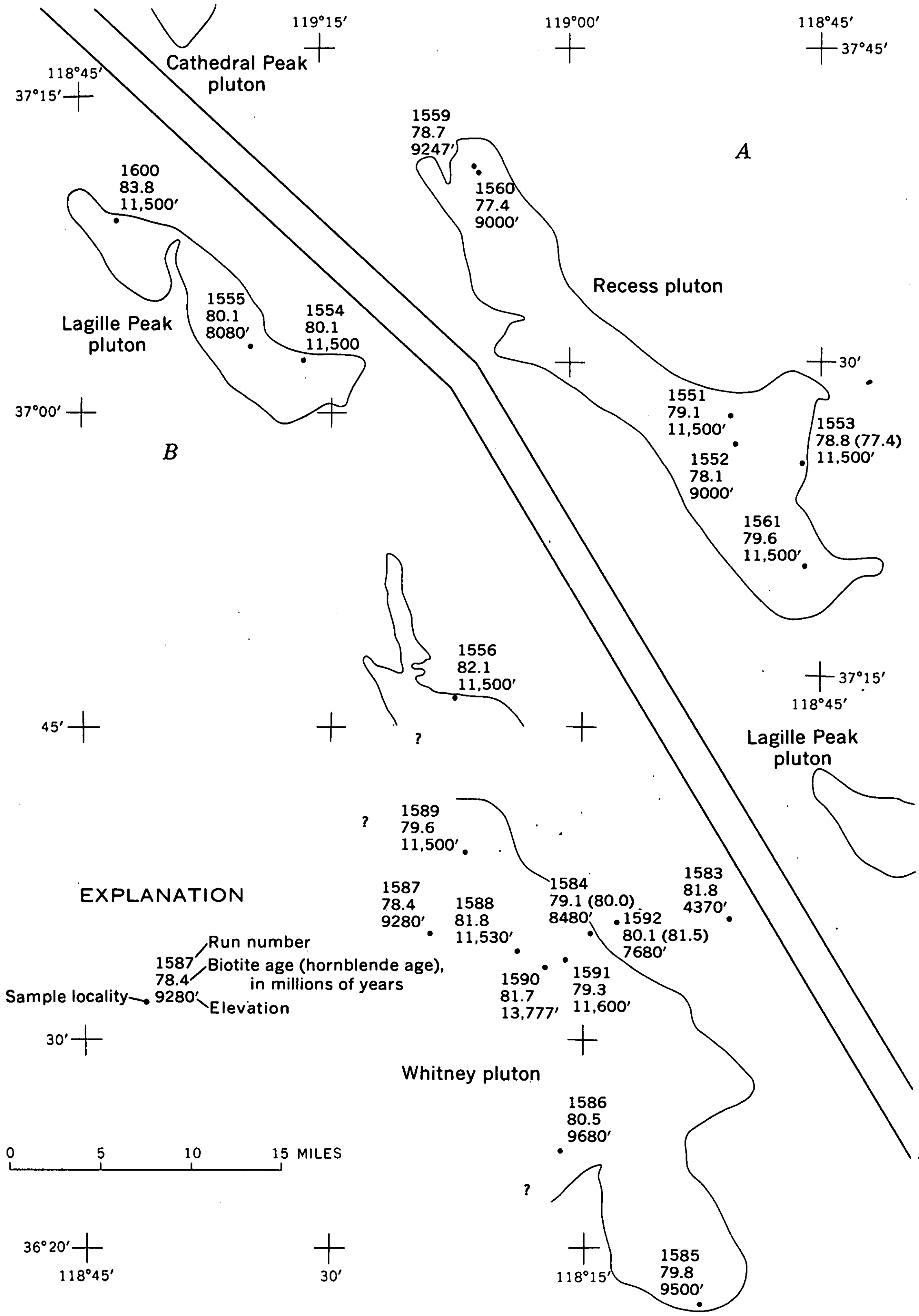

FIGURE 3.—Potassium-argon dates on samples from plutons of Cathedral Peak type. *A*, Recess pluton; *B*, Whitney pluton.

The data from the Lagille Peak pluton (fig. 3) are too limited to warrant detailed analysis.

The pattern of ages in the Whitney pluton is not well placed for a study of the relation between age and potassium content, since the samples were selected to investigate age as a function of position. Only subsequent to sample collection did the results from the Cathedral Peak pluton become available.

If the absolute age data obtained in the Whitney pluton are interpreted in terms of dipping isochronal surfaces, a correlation between east-west position, elevation, and age appears—the isochrons dipping about 7° westward and having a perpendicular separation of about 600 feet for a time difference of 1 m.y. This conclusion is based upon a somewhat arbitrary analysis of the data, but it is interesting that this part of the Sierra is thought to have had much greater uplift and associated erosion than the area to the north (the general absence of roof pendants being considered significant). If relative uplift and erosion have been measured in thousands of feet, the appearance southward of age as a function of elevation is not surprising. It is concluded that there is no linear trend in the order of emplacement of the Cathedral Peak type plutons but that there is an increasing dependence of age upon elevation southward (for Cathedral Peak pluton, no observable change in age for 4,000 ft; Recess pluton, 1 m.y. per 2,000 ft; Whitney pluton, 1 m.y. per 600 ft).

Three biotite-hornblende pairs support the conclusion that several millions of years were involved in the emplacement of these quartz monzonite plutons: KA 1533 (82.5 m.y.) and KA 1533–HBD (84.3 m.y.) from the Cathedral Peak pluton; KA 1553 (78.8 m.y.) and KA 1553–HBD (77.4 m.y.) from the Recess pluton; and KA 1584 (79.1 m.y.) and KA 1584–HBD (80.0 m.y.) from the Whitney pluton. The internal agreement of each pair implies real significance for the age indicated by each pair, and the spread of mean ages of the three pairs implies real differences in the age of each pluton.

DEPTH OF EMPLACEMENT OF THE SIERRAN PLUTONS

The data we shall use to determine the depth of emplacement of the Sierran plutons are the data on the relation of age to elevation in the Cathedral Peak-type plutons. Such an approach to evaluating depth of emplacement must be based upon a heat model of granite emplacement and cooling. We are at once upon uncertain ground. But if the tenuousness of the fabric being woven is fully appreciated, no harm results from such discussions, and possibly some useful ideas may result.

The required parameters of the problem are several. First, one must assume the existence and value of a steady-state temperature gradient. This can be generated either by radioactivity within the upper 25 km of the crust or by a heat source below the upper layers. As it will not make any particular difference in the results, the latter model is chosen because of its ease of handling. A maximum of 33°C per km and a minimum of 25°C per km are suggested by heat flow and borehole data as limits of permissible gradients. For reasons discussed below, the gradient is achieved by holding the temperature constant at 800°C at the appropriate depth. If we consider that the data previously obtained on argon diffusion in phlogopite and glauconite by Evernden, Curtis, Kistler, and Obradovich (1960) are relevant to biotite under a load of several kilometers, some conclusions are immediately possible. First of all, note that one of the figures given in this earlier work is not correct. As pointed out by Paul Damon, the appropriate time interval to go with the listed f values is 10^6 years rather than 10^5 years. Therefore, an f value of 0.4 is to be associated with 325°C for biotite grains with a significant diffusion dimension of 1 millimeter. Since the significant diffusion dimension for biotite grains of Sierran rocks is probably less than 1 millimeter, 325°C is certainly beyond the temperature range at which rocks of nearly the same age could remain for 2 to 3 m.y. and still display differences in age on the order of a few million years. With a surface temperature of 30°C, the 300°C isotherm of the model is pertinent. Factors inconsistent with emplacement of these plutons at depths where the ambient temperature is 325°C are the biotite age differential between the southern end of the Cathedral Peak pluton and the north end of the Recess pluton; the concordance of the biotite-hornblende pair from KA 1533 (Cathedral Peak pluton); and the lack of any dependence of age upon elevation in the Cathedral Peak pluton. The levels now exposed of these pluton ends were certainly at the same depth at all times since emplacement of the younger. If they were ever both at 325°C at the same time, they would certainly show essentially identical ages today, would probably display discordant biotite-hornblende ages, would display age as a function of elevation, and the two ends of the Cathedral Peak pluton would not show different apparent ages. Thus, on the argument of geothermal gradient alone, the maximum permissible depth for the top of the plutons is less than 12 km for 25°C per km, or 9 km for a gradient of 33°C per km.

What is the temperature of a pluton at the time of "initiation of cooling"? We shall not attempt to discuss the period of time involved in emplacement of a pluton or the temperature history during that time. We presume that we can establish a temperature distribution of approximately the correct type for the period when cooling became the ruling heat process. The model will be designed to err on the side of a low estimate of heat in the pluton after "initation of cooling" so that the estimate of depth of emplacement will be a maximum.

The geologic thermometer used to establish the temperature at time of "initiation of cooling" is the mineral assemblage found in roof pendants, zenoliths, and metamorphic aureoles of the plutons. Bateman, Clark, Huber, Moore, and Rinehart (1963) can be consulted for a discussion of these metamorphic rocks and their mineral assemblages. The essential feature is that they are predominantly hornblende hornfels with a small percentage of pyroxene hornfels, and locally display both wollastonite- and calcite quartz-bearing phases as well as andalusite- and sillimanite-bearing phases. Therefore, the mean temperature condition during the genesis of these rocks was in the pressure-temperature region where the three phase boundaries of figure 4 intersect. The andalusite-sillimanite data (Weill, 1966) are essential to the argument. The calcite quartz-wollastonite data are from Ellis and Fyfe (1956) and the pyroxene hornfels-hornblende hornfels curve is from Fyfe, Turner, and Verhoogen (1958). The PH-HH curve is hypothetical and can move appreciably in response to varying total composition of the rock, but it is thought to be at very nearly the correct position for rocks of granitic composition. The conclusion is that a temperature of approximately 600°C is predicted for rocks forming near these phase-boundary intersections. Since such a temperature implies that the granitic mass was largely crystalline at this time, heat of crystallization can be disregarded.

The heat model at time of "initiation of cooling" is then 800°C (800°C is adequate, as this is well above 600°C) held constant at the appropriate depth, geothermal gradient to 600°C, 600°C to depth D below the surface, and a uniform gradient to the surface (fig. 5*A*). No account is taken of lateral cooling, for the Cathedral Peak pluton and the surrounding portions of the Half Dome pluton show no lateral variations in age. The ages in the Half Dome pluton near the contact with the Cathedral Peak pluton are indistinguishable from those of the Cathedral Peak pluton, and the dates within the latter are uniform from edge to edge. The final step is to cool this mass to the geothermal gradient by conduction without introduction of additional heat. As can be seen, every theoretical departure from the actual environment is probably in the direction of underestimating heat available. The computations were carried through for several values of D (depth of emplacement). Figure 5*B* shows the position of the 300°C isotherm as a function of D, depth of emplacement; d, depth into the pluton; and t, time in 10^6 years since initiation of cooling.

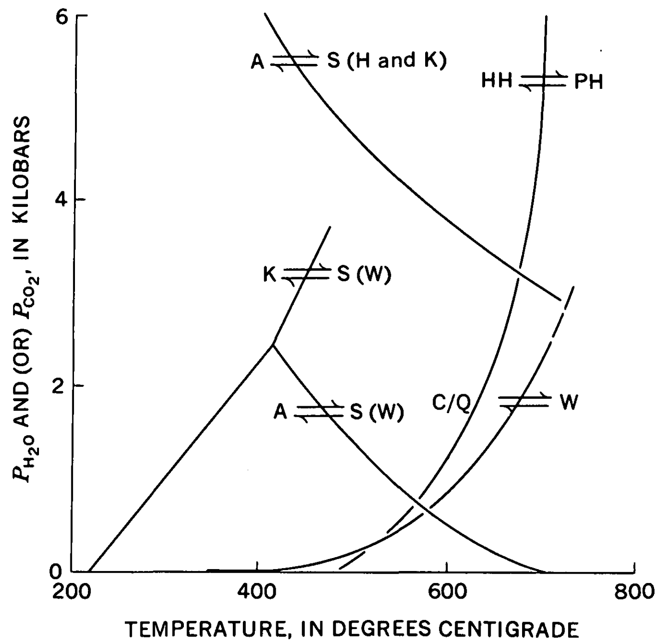

EXPLANATION

Kyanite-sillimanite-andalusite (K–S–A) curves. Curves from Weill (1966) are designated (W); curve from Holm and Kleppa (1966) is designated (H and K).
Wollastonite-calcite/quartz (W–C/Q) curve from Ellis and Fyfe (1956).
Pyroxene hornfels-hornblende hornfels (PH–HH) curve from Fyfe, Turner, and Verhoogen (1958).

FIGURE 4.—Pressure-temperature fields for metamorphic mineral and rock pairs.

We will use the 300°C of our model as our guide temperature for the reasons stated. We will also assume that the pattern of movement of this isotherm in the cooling pluton is reflected quite closely in the pattern of age in relation to elevation in the pluton today. In the discussion which follows, figures not in parentheses refer to a 33°C per km gradient; figures in parentheses refer to a 25°C per km gradient. Note first the data for $D=8(11)$ km. At the top of the pluton, the 300°C isotherm subsides 0.7 km in 10^6 years (0.7 km in 1.8×10^6 years). At greater depth (the tops of all the plutons are now eroded), this isotherm subsides more slowly. Assuming the validity of the assumption made above, it can be stated that a pluton emplaced at 8(11) km depth must show age as a function of elevation at least to the level 10^6 years within 2,000 feet (1.8×10^6 years within 2,000 feet). Such is not observed in the Cathedral Peak pluton and so such values of D are inadmissible.

For $D=4$ (5.5) km, age as a function of elevation at the top of the pluton is predicted to be 0.6×10^6 years within 1.8 km (1.1×10^6 years within 1.8 km), while at 2.5 km depth within the pluton ($d=2.5$) a rate of 10^6 years within 1.4 km (1.8×10^6

359-835 O—69——3

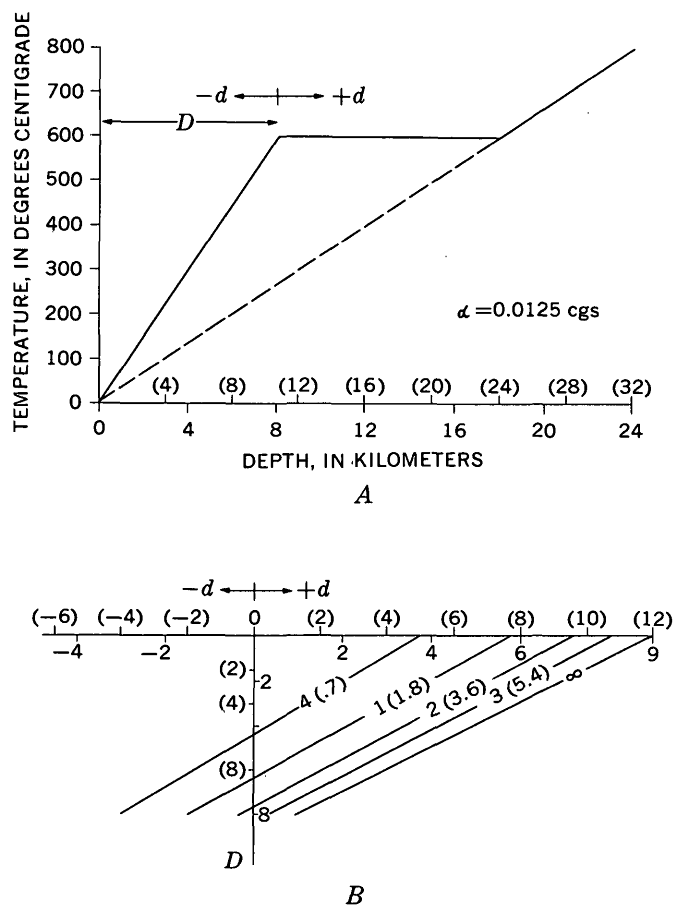

FIGURE 5.—Heat model for intrusive rocks of the Sierra Nevada. Numbers in parentheses refer to a 25°C per km geothermal gradient. Numbers not in parentheses refer to a 33°C per km geothermal gradient. *A*. Assumed temperature distribution at "initiation of cooling" and geothermal gradient. *B*. Position of 300°C isotherm as function of *d* (depth into pluton), *D* (depth of emplacement), and *t* (time in 10^6 years since "initiation of cooling").

years within 1.4 km) is predicted. Whether a *D* of 4 km is admissible depends upon the depth of erosion of the pluton today. In any case, a *D* of 6 km is inadmissible on this model. Note that the suggested gradients in the Recess and Whitney plutons can be found on the profile for $D=5$ km or less at values of *d* of a very few kilometers. Thus, the entire pattern of observed gradients can be explained by intrusion to depths of 5 km or less and subsequent pronounced tilting of the batholith. Such tilting has often been invoked to explain the lack of roof pendants in the Mount Whitney area.

Is this prediction of shallow emplacement supported or denied by other data? Broad-scale field investigations tend to support such shallow depths of emplacement because of the demonstrably short interval of geologic time between emplacement and unroofing by erosion of such plutons and because of the known thickness of sediments which accumulated as a result of erosion between the time of emplacement and exposure of the plutons (Curtis and others, 1958). Bateman, Clark, Huber, Moore, and Rinehart (1963) have argued for a depth of emplacement of Sierran plutons of 15 km, basing their arguments on the mineralogy of the metamorphic and igneous rocks. As regards the metamorphic rocks, the present uncertainties in position of the plotted sillimanite-kyanite-andalusite triple point make impossible any detailed conclusions on temperature and depth of emplacement of these plutons based upon position of this triple point. Reference should be made to the article by Holm and Kleppa (1966) in which the various computed positions of the sillimanite-kyanite-andalusite phase boundaries are plotted. The phase boundaries as plotted by Weill (1966) agree nicely with our heat-flow analysis. The essential point for our analysis is the intersection of the sillimanite-andalusite and the wollastonite-calcite/quartz curves. Based on Weill's data, a temperature of approximately 600°C and a $P_{H_2O}=P_{CO_2}$ of 0.8 kilobars are predicted as the temperature-pressure conditions for genesis of the observed metamorphic mineral assemblages in the Sierra Nevada. If P_{H_2O} is presumed to be equal to P_{load}, a depth of emplacement of 3 km is predicted, whereas if P_{H_2O} is hydrostatic, a depth of 8 km is predicted. Therefore, there is no conflict with the depths predicted by the heat-flow model. The data of Holm and Kleppa, together with the wollastonite-calcite/quartz data of Ellis and Fyfe (1956), predict that the temperature-pressure conditions necessary for genesis of these rocks are 700°C and 3 kb. At present, we see no obvious way to decide on the relative merits of the investigations of Weill (1966) and Holm and Kleppa (1966). The conclusion must be that the mineralogical data predict temperatures between 600°C and 700°C and pressures of 0.8 to 3.0 kb with no more refined specification possible. Bateman's argument based upon the composition of the granitic rocks has two flaws well known to him. First, it was necessary to argue about the anorthite-albite-orthoclase system while possessing only data on the albite-orthoclase system. For this reason, one cannot evaluate the soundness of his argument as applied to granites of the Sierra Nevada area. Secondly, much crystallization may well have taken place prior to final emplacement of the pluton. Therefore, we can state that neither of Bateman's thermometers is sufficiently well calibrated to allow prediction of depth of emplacement of the Sierran plutons. There is no clear demonstrable disagreement of the mineralogical data with our conclusions.

DISCORDANT BIOTITE-HORNBLENDE PAIRS—EVIDENCE OF REHEATED PLUTONS

The gross discordances in potassium-argon ages of biotite-hornblende pairs from specimens of granitic rock found by Kistler, Bateman, and Brannock (1965) on the east side of the Sierra Nevada and further data in this report are clear evidence that old granitic rocks (180–210 m.y.) were reheated by much younger plutons (90–80 m.y. old).

The numerous discordant samples reported by Kistler, Bateman, and Brannock (1965) are shown on plate 2. The samples that displayed marked discordance (greater than 5 m.y.) in the present study are given in the following table.

Samples in present study that show discordance greater than 5 m.y.

Run	Mineral	Age (m.y.)	(x−y) (percent)	Remarks
KA 1432	Biotite	128	0.6	West of "Upper Cretaceous" plutons.
1432	Hornblende	142	.4	Do.
1511	Biotite	97	.1	Do.
1511–HBD	Hornblende	125	.7	Do.
1519	Biotite	92	.3	
1519–HBD	Hornblende	100	.7	
1540	Biotite	89	.0	
1540–HBD	Hornblende	97	.6	
1564	Biotite	89	.2	Marked discordance in all minerals from this rock.
1564–HBD	Hornblende	96	.9	Do.
1582	Biotite	74	.9	Walker Pass.
1582–HBD	Hornblende	86	.5	Do.
1601	Biotite	83	.5	Lamarck Granodiorite, reheated by Recess pluton.
1601–HBD	Hornblende	88	.8	Do.
1609	Biotite	87	.3	Discordance due to depth of emplacement and (or) erosion?
1609–HBD	Hornblende	93	.1	
1626	Biotite	94	.5	
1626–HBD	Hornblende	101	.6	
1628	Biotite	104	.4	West of "Upper Cretaceous" plutons.
1628–HBD	Hornblende	144	.2	
1632	Biotite	152	.1	
1632–HBD	Hornblende	162	.1	
1633	Biotite	89	.0	
1633–HBD	Hornblende	120	2.0	
1634	Biotite	144	.3	
1634–HBD	Hornblende	156	.9	
1635	Biotite	125	.1	
1635–HBD	Hornblende	148	.1	
1680	Biotite	61	.6	Southern California.
1680–HBD	Hornblende	72	.7	
1698	Biotite	108	.1	West of "Lower Cretaceous" plutons.
1698–HBD	Hornblende	140	.7	
1699	Biotite	117	.0	
1699–HBD	Hornblende	140	.4	
DKA 1029	Biotite	85		East of "Upper Cretaceous" plutons.
MKA 409	Hornblende	95		
DKA 1031	Biotite	83		
1032	Hornblende	93		
1030	Biotite	99		East of "Upper Cretaceous" plutons.
MKA 410	Hornblende	206		
KA 487	Biotite	88		
MKA 458	Hornblende	97		
61019	Biotite	149		
61025	Hornblende	158		
71022	Biotite	86		
61196	Hornblende	101		
71083	Biotite	91		San Marcos Gabbro.
71067	Hornblende	101		

The argument of this section and the following ones will depend strongly upon the data of Hart (1964). Hart demonstrated the concordance of biotite and hornblende ages can indicate either initial cooling or degassing of both minerals by a later event. Concordance does imply a heating-cooling event, however. The pattern of discordance displayed by Hart's data is extremely important. The biotite, along the profile sampled by Hart, lost all of its argon before the hornblende indicated other than the uncertain indication of a 15 percent loss at great distance. Thus the pattern of discordance expected along a profile of reheating in the older mass will not be one showing near-concordance of biotite and hornblende at all distances, the age changing gradually from older to younger, but rather concordance beyond the effect of the younger pluton, with increasing discordance until the biotite reaches the age of the younger pluton, and only there, or farther on toward the younger intrusive, the decrease of hornblende ages to concordance with the biotite age. A series of ages such as that at "A" on plate 2 is the expected result of reheating by a single later event. In that area, the older rocks are to the west, the younger to the east. The sequence of determined ages from west to east, that is, towards the younger intrusive is:

Run	Age (m.y.) Biotite	Hornblende
KA 1700		138
1699	117	140
1698	108	140
1683	102	100

Field evidence and lithology of sample KA 1683 suggest that it is from the older granites (more acidic than rocks to east, evidence of extensive recrystallization, deuteric alteration of most minerals, and strong distortion of biotites). Reheating with consequent argon loss is clearly shown in the series at "B" on plate 2 and by numerous other samples on the western side of the Sierra.

CONCORDANT BIOTITE-HORNBLENDE PAIRS—EVIDENCE OF THE AGE OF AN INTRUSIVE EVENT

We shall classify as concordant those pairs of ages which agree to within 5 m.y., such a degree of concordance being interpreted to mean that the pair of ages quite closely date an intrusive event, either that of the rock dated or that of an adjacent intrusive. In order of determined age, the concordant pairs are as follows:

Run	Age (m.y.) Biotite	Hornblende
KA 1553	79	77
1584	79	80
1667	80	81
61001, 61020	80	83
KA 1592	82	83
1533	83	84
1538	83	84
9*	83	88
KA 1508	88	84
71077, 71065	86	88
21*	87	84
14*	85	87
13*	87	86
KA 1575	86	88
1610	88	86
488, 61192	88	86
1605	87	90
1539	90	89
1516	87	90
1514	88	91
FD 13†	90	90
6*	92	91
KA 1568	92	96
1678	93	98
61007, 61018	94	90
KA 1541	95	98
71079, 71073	94	95
KA 1512	97	98
71075, 71061	94	95
KA 1570	98	102
71081, 71071	98	102
KA 1683	101	100
1629	103	105
1509	105	105
1506	101	106
1569	102	108
1630	114	115
1502	121	121
1438, 1439	126	131
1440, 1441	129	132
1436, 1437	132	136
1624	138	136
1701	143	146
1664	145	148
1702	153	150
61008, 61026	210	206

*Sample numbers from Kistler, Bateman, and Brannock (1965).
†Sentinel granodiorite from Kistler and Dodge (1966).

The greater number of ages within the range 80 to 108 m.y. is largely the result of the sampling pattern and is not to be considered significant in interpretation. Rather, the distribution of rocks according to age groups as shown on plate 1 is a more accurate estimate of the relative significance of each age interval in the genesis of the batholith. These data show that no concordant pair of ages is lacking for any significant time interval after an age of 150 m.y. Certainly, there are two periods of 10 million years for which there are no ages, but the chances seem good that those intervals could be filled by selective sampling. The concept of several distinct periods of granite emplacement separated by long intervals of no granite emplacement (Curtis and others, 1958; Kistler and others, 1965) is not supported by the total body of potassium-argon ages. A more reasonable interpretation of the mineral age data is that granite emplacement in the environs of the Sierra Nevada was an essentially continuous process covering the period from 210 m.y. ago up to approximately 80 m.y. ago. As will be discussed below, the volume of granite emplaced in equal intervals of time was probably grossly different and the pulses of orogeny that geologists have defined in this area seem to be culminations of activity of a basically continuous process.

Therefore, the two areas of granitic terrane—eastern Australia and the Sierra Nevada—in which ages have been reasonably well studied on a broad scale yield the same answer. Granite genesis and emplacement can be a nearly continuous process for more than 100 m.y. It will be shown below, however, that the continuity of emplacement of plutons in the Sierra Nevada is actually the result of a series of pulses of granite genesis and emplacement which yield a continuous series of ages because of complex mechanical and thermal histories. The spacing of the pulses and the time required for the completion of each give the continuity of concordant potassium-argon ages.

GROWTH OF THE SIERRA NEVADA BATHOLITH

We here consider the pattern of ages obtained by all techniques throughout the Sierra Nevada and its environs in order to clarify the preceding discussions of continuity in magmatic activity during the Mesozoic Era. The total body of data available, including ages obtained by potassium-argon, rubidium-strontium, and lead-alpha methods indicates that five major epochs of intrusion by granitic magma occurred from the Middle Triassic to the Late Cretaceous at intervals of approximately 30 million years. We identify each epoch by numerical age representing the oldest known age correlated with that epoch; they are in the sequence 210, 180, 148, 121, and 90 m.y. Distinctly mappable granitic rock series that were emplaced during each of these intrusive epochs have been well defined in California by comprehensive work in different areas by several field geologists (Calkins, 1930; Bateman and others, 1963; Kistler, 1966b). We shall first discuss the distribution of ages shown by all methods in these well-known areas (see outlined area, pl. 1) and then extrapolate to other areas on the basis of our potassium-argon data on biotite and hornblende.

CATHEDRAL RANGE INTRUSIVE EPOCH OF LATE CRETACEOUS AGE

The Cathedral Range intrusive epoch is here defined as the time of emplacement of granitic rocks of the Tuolumne Intrusive Series. This is the younger of two series of granitic rock in the Yosemite region of the Sierra Nevada that were defined by Calkins (1930). The younger series includes the Sentinel Granodiorite, Half Dome Quartz Monzonite, Cathedral Peak Granite and Johnson Granite porphyry. Subsequent mapping by other investigators has shown that rocks of the Tuolumne Intrusive Series occur along the crestal regions of the Sierra Nevada for its entire length (Mayo, 1941; Bateman, 1961; Broderson, 1962) and that these rocks represent the youngest intrusions in the batholithic complex. Dates for rocks of the Tuolumne Intrusive Series have been obtained by the potassium-argon method using mineral separates (Curtis and others, 1958; Kistler and others, 1965; Kistler and Dodge, 1966; and many more determinations in this report), by rubidium-strontium isotope analyses of whole rocks (Hurley and others, 1965) and by the lead-alpha method (Jaffe and others, 1959; Bateman and others, 1963). The maximum age for the oldest member of the series, the Sentinel Granodiorite, by concordant potassium-argon dates on hornblende, biotite, and orthoclase from the same specimen of rock, is 90 m.y. (Kistler and Dodge, 1966). The lead-alpha age of uranothorite from the Half Dome Quartz Monzonite, the next younger member of the series, is 88 m.y. (Jaffe and others, 1959); ages on zircons from the Lamarck and Round Valley Peak Granodiorites are 91 and 88 m.y., respectively (Bateman and others, 1963). According to Hurley, Bateman, Fairbairn, and Pinson (1965), a rubidium-strontium whole-rock isochron of 90 m.y. can be constructed with the analyzed specimens of the Mount Givens and Lamarck Granodiorites and later quartz monzonites from this series. All of the age data together indicate that the first increment of magma of the Tuolumne Intrusive Series was intruded 90 m.y. ago. The spread of concordant mineral ages from 90 m.y. to 79 m.y. is the maximum interval of time available for the intrusion of the tremendous volume of magma represented by these rocks and for the cooling of this mass to a temperature low enough to permit equal retention of radiogenic argon in biotite and hornblende (about 300°C, see page 12). Some of the spread in ages is due to the mechanisms discussed in other sections of this paper, but ages of mineral pairs from rocks emplaced during the Cathedral Range intrusive epoch are generally concordant and date the event as Late Cretaceous.

HUNTINGTON LAKE INTRUSIVE EPOCH OF EARLY CRETACEOUS AGE

The Huntington Lake intrusive epoch is here defined as the time of emplacement of the granitic rocks represented by the granodiorite of "Dinkey Creek" type in the Huntington Lake area, Fresno County, Calif. and correlative intrusive rocks elsewhere. The granodiorite of "Dinkey Creek" type mapped by Krauskopf (1953), Macdonald (1941), and Hamilton (1956) without delineation of individual plutons is a series of rocks ranging in composition from quartz diorite to quartz monzonite. The granodiorite of "Dinkey Creek" type in the vicinity of Huntington Lake is known from contact relationships to be older than the Mount Givens Granodiorite (Bateman and others, 1963). In the area where the "Dinkey Creek" type has been mapped, the maximum potassium-argon age of hornblende, determined from a quartz diorite at its westernmost exposure, is 115 m.y., and the biotite-hornblende pairs from dated specimens generally have discordant ages (Kistler and others, 1965). Ages approach concordance (KA 1630) and a maximum only in specimens collected far from the contact between the granodiorite of "Dinkey Creek" type and rocks of the Tuolumne Intrusive Series to the east. A whole-rock rubidium-strontium isochron for a granodiorite of "Dinkey Creek" type exposed near Huntington Lake yields an age of 104 m.y. (fig. 6*A*; table 4).

Other granitic rocks intruded during the Huntington Lake intrusive epoch include some of the plutons in the southern California batholith and those in the Santa Lucia Mountains of the so-called Coast Range batholith. The rubidium-strontium whole-rock age for the Santa Lucia plutons is 117 m.y. (fig. 6B; table 4). Banks and Silver (1966) report isotopic uranium-lead ages between 109 and 116 m.y. for zircons from plutons in the southern California batholith. All the geochronologic data show that the Huntington Lake intrusive epoch spans the time interval 121 m.y. to 104 m.y. ago and is Early Cretaceous in age.

YOSEMITE INTRUSIVE EPOCH OF LATE JURASSIC AGE

The Yosemite intrusive epoch is here named for the time of emplacement of granitic rocks exposed in Yosemite Valley—its type area. These rocks include the biotite granite of Arch Rock, granodiorite of The Gateway, El Capitan Granite, and Taft Granite. It includes the so-called biotite granite series of the Yosemite Valley, which Calkins (1930, p. 121) dated as older

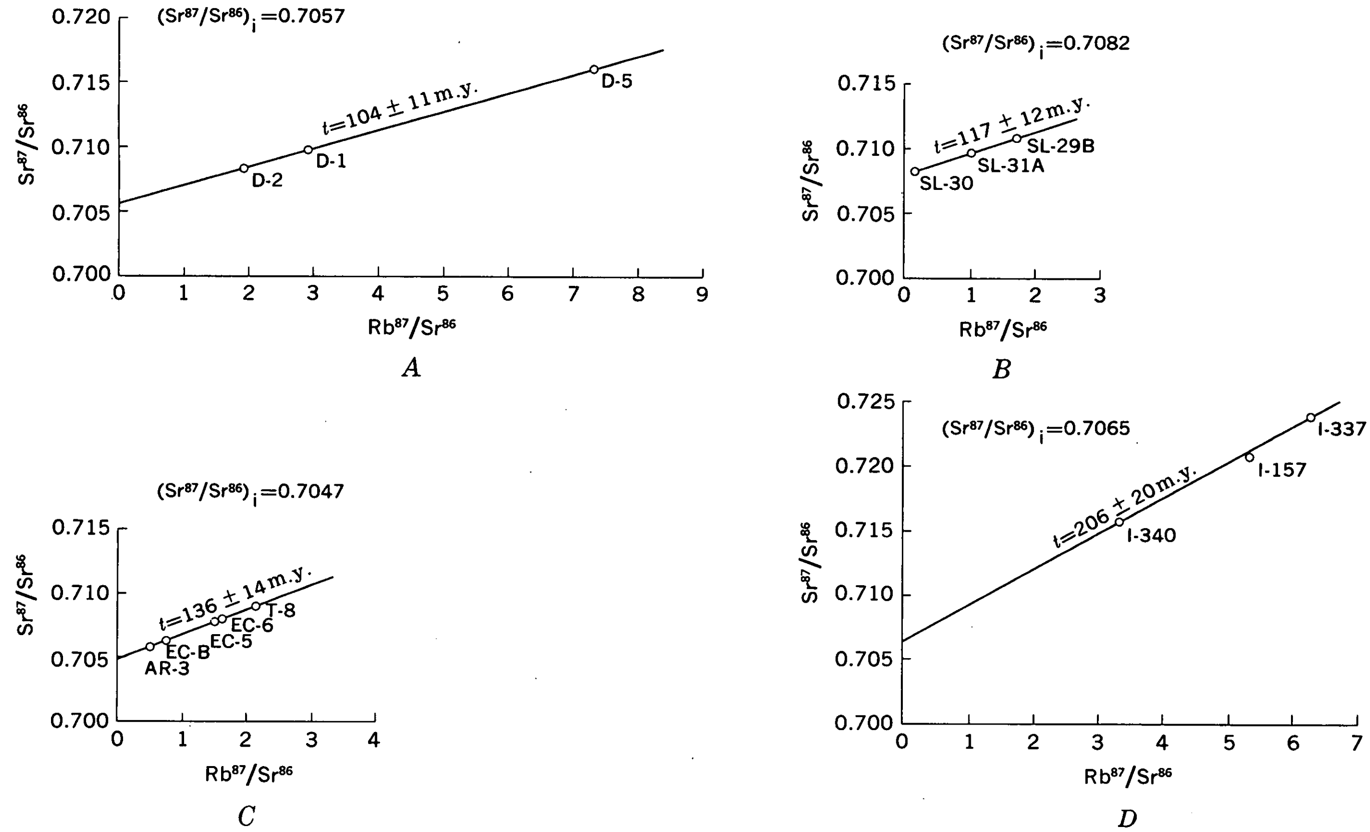

FIGURE 6.—Rubidium-strontium isochron plots for granitic rocks in California. *A*. Granodiorite of "Dinkey Creek" type. *B*. Plutons of Santa Lucia Mountains. *C*. Granitic rocks of the Yosemite intrusive epoch. *D*. Quartz monzonite of Lee Vining Canyon. (Analytical uncertainty does not include the uncertainty in the Rb^{87} decay constant.)

than his Tuolumne Intrusive Series because the Sentinel Granodiorite of the Tuolumne intrudes the El Capitan Granite.

Age determinations of rocks intruded during the Yosemite intrusive epoch have been obtained by potassium-argon analyses of biotite and hornblende (Curtis and others, 1958, and this report) and by rubidium-strontium isotopic analyses of whole rocks. The maximum mineral age (101 m.y.) for this series in the type area is for hornblende from a specimen collected at the most westerly outcrop of granodiorite of The Gateway (KA 1663), but rubidium-strontium analyses of whole-rock specimens of biotite granite of Arch Rock, El Capitan Granite, and Taft Granite yield an isochron of 136 m.y. (fig. 6*C*; table 4). The data suggest that the mineral ages from specimens in the Yosemite Valley area have all been reduced by various amounts by reheating during the later intrusions of the Tuolumne Intrusive Series to the east and the granodiorite of "Dinkey Creek" type to the south. The rubidium-strontium age indicates the biotite-granite series of the Yosemite Valley to be a temporal equivalent of the Late Jurassic granitic rocks of the foothill belt to the west. The foothill granitic rocks generally have concordant biotite-hornblende potassium-argon ages between 148 and 136 m.y. (KA 1624), etc. All the geochronologic data show that the Yosemite intrusive epoch spans the time interval 148 to 132 m.y. ago and is Late Jurassic in age.

INYO MOUNTAINS INTRUSIVE EPOCH OF EARLY AND MIDDLE JURASSIC AGE

The name Inyo Mountains intrusive epoch is here assigned to the period of time when the majority of the plutonic rocks exposed in the Inyo and White Mountains and the Tinemaha Granodiorite and granodiorite of McMurray Meadows exposed in the Sierra Nevada were emplaced (Bateman, 1961; McKee and Nash, 1967). The Lamarck Granodiorite intruded during the Cathedral Range intrusive epoch is known from contact relationships to be younger than the Tinemaha Granodiorite in the area of exposures near the crestal region of the Sierra Nevada southwest of Big Pine, Calif. (Bateman, 1961).

Age determinations of rocks intruded during this epoch are from potassium-argon analyses of biotite and hornblende (Kistler and others, 1965; McKee and Nash, 1967; this report) and from lead-alpha ages of zircons

TABLE 4.—*Rubidium-strontium analytical data*

[Santa Lucia Mountains samples analyzed by R. W. Kistler; all other analyses by Carl E. Hedge]

Sample		Rb (ppm)	Sr(total) (ppm)	Rb^{87}/Sr^{86}	Sr^{87}/Sr^{86}*
LEE VINING INTRUSIVE EPOCH					
1–340	Quartz monzonite of Lee Vining Canyon.	160	140	3. 31	0. 7160
357	do	156	85. 8	5. 28	. 7211
337	do	185	86. 3	6. 21	. 7243
YOSEMITE INTRUSIVE EPOCH					
Ar–3	Biotite granite of Arch Rock.	[1] 80. 6	[1] 448	0. 52	0. 7056
EC–B	do	[1] 84. 6	[1] 313	. 78	. 7061
5	El Capitan Granite.	[1] 127	[1] 240	1. 54	. 7075
6	do	[1] 127	[1] 223	1. 65	. 7076
T–8	Taft Granite	[1] 148	[1] 197	2. 18	. 7088
HUNTINGTON LAKE INTRUSIVE EPOCH					
D–1	Granodiorite of "Dinkey Creek."	208	208	2. 90	0. 7098
2	do	[1] 173	[1] 264	1. 91	. 7085
5	do	[1] 270	[1] 107	7. 31	. 7162
SANTA LUCIA MOUNTAINS, MAIN JUNIPERO SERRA PLUTON					
SL–30	Biotite-hornblende gabbro.	22. 8	761	0. 09	0. 7082
31A	Biotite- granodiorite.	[1] 149	[1] 427	1. 02	. 7099
29B	Aplite	[1] 175	[1] 302	1. 68	. 7109

*Sr^{87}/Sr^{86} corrected for fractionation by normalizing observed Sr^{86}/Sr^{88} ratios to 0.1194.
[1] Rubidium and strontium concentrations by isotope dilution. All other concentrations by X-ray fluorescence. Constants:

$$Rb^{87}: \lambda_\beta = 1.39 \times 10^{-11} yr^{-1}$$

0.283 g/g Rb

$Sr^{87}/Sr^{86} = \pm 0.0010$ at 95 percent confidence level for a single analysis. Rubidium and strontium concentrations by isotope dilution are ±2.0 percent. Rubidium-strontium ratios determined by X-ray fluorescence are ±3.0 percent. Rock ages derived from the isochrons are ±10 percent owing to analytical uncertainty and to the small spread of Rb/Sr ratios in most of the series investigated.

(Ross, 1965). Potassium-argon ages of biotite-hornblende pairs from most specimens are grossly discordant. The zircon ages, however, cluster around 180 m.y. and the maximum hornblende age is 183 m.y. (Kistler and others, 1965; Ross, 1965). Thus an age of approximately 180 m.y. is considered to mark the time of earliest intrusion by magma within this event. As in the other older granitic rocks, mineral ages of rocks of the Inyo Mountains intrusive epoch become more reduced and discordant with proximity to the Late Cretaceous granitic rocks near the crest of the Sierra Nevada. Hornblende potassium-argon ages indicate the Inyo Mountains intrusive epoch spans the time interval from 180 to 160 m.y. ago and is Early and Middle Jurassic in age.

LEE VINING INTRUSIVE EPOCH OF MIDDLE AND LATE TRIASSIC AGE

The Lee Vining intrusive epoch is here assigned to the period of time during which granitic rocks that include the granodiorite of Mono Dome and the quartz monzonite of Lee Vining Canyon that are exposed to the east of the Tuolumne Intrusive Series in the Sierra Nevada and in the vicinity of Mono Lake were emplaced (Kistler, 1966a, 1966b). The Late Cretaceous quartz monzonite of Aeolian Buttes intrudes the quartz monzonite of Lee Vining Canyon in exposures west of Grant Lake in the June Lake Loop (Kistler, 1966a). We have also seen a porphyritic granodiorite intruded during the Lee Vining intrusive epoch that is intruded by an equigranular quartz monzonite of the Inyo Mountains intrusive epoch in Blind Spring Hill, due west of the northern end of the White Mountains.

Maximum biotite and hornblende potassium-argon ages for rocks in this series are 210 m.y. (61008, 61026) and rubidium-strontium whole-rock analyses yield an isochron of 206 m.y. for specimens of the quartz monzonite of Lee Vining Canyon (fig. 6*D*, table 4). Biotite and hornblende ages of these Middle Triassic granitic rocks are reduced and grossly discordant in specimens collected near the Tuolumne Intrusive Series in the Sierra Nevada (DKA 1030, MKA 410); the ages are maximum and concordant in specimens from exposures south of Mono Lake (61008, 61026). The geochronologic data indicate the Lee Vining intrusive epoch spans the time interval from 210 m.y. to 195 m.y. ago and is Middle and Late Triassic age.

SUMMARY OF AGES IN ALL INTRUSIVE EPOCHS

The potassium-argon mineral ages and whole-rock rubidium-strontium ages that have been discussed are projected onto diagrammatic sections that show the intrusive epochs of the batholithic rocks across California (figs. 7, 8). Potassium-argon "ages" of all mineral systems from the specimens of older rock plutons may be reduced near contacts with succeeding younger intrusive bodies. In all of the older rocks, however, samples have been collected sufficiently distant from younger intrusive rocks to insure that the minerals of the older rocks have had practically complete retention of all radiogenic argon generated since their initial cooling, as shown by their concordant and older ages. Ages of biotite-hornblende pairs from plutons intruded during the Cathedral Range intrusive epoch are generally concordant. Maximum concordant ages of mineral pairs in all the intrusive epochs are in close agreement with either the whole-rock rubidium-strontium age of rocks of the intrusive epoch or with uranium-lead age of zircons of the epoch. These maximum ages are taken to mark the beginning of each of the five epochs of plutonism in the

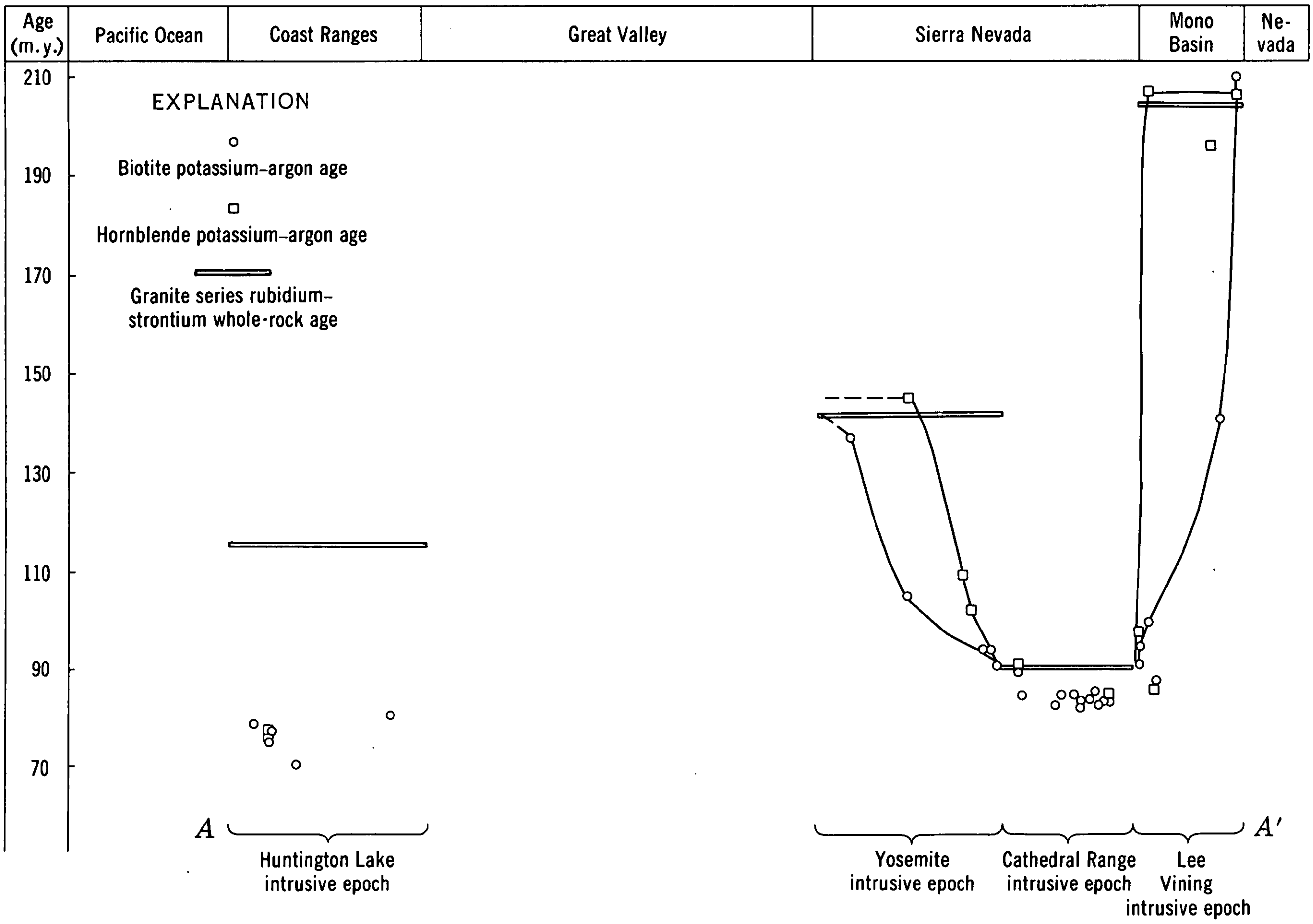

FIGURE 7.—Potassium-argon mineral ages and rubidium-strontium whole-rock ages for granitic rocks of the Lee Vining, Yosemite, Huntington Lake, and Cathedral Range intrusive epochs projected to a diagrammatic cross section of California. Location of cross section shown on plate 2.

Sierra Nevada and environs. The data on concordant biotite-hornblende ages show that the intrusive process takes 10 to 20 million years for a given epoch, thus explaining the near continuum of granite emplacement indicated by the concordant potassium-argon mineral ages.

Analysis of the entire body of potassium-argon dates of this report suggests the distribution of outcrops of rocks of the five intrusive epochs as outlined on plate 1. In some areas, an assignment of granitic rocks to a specific epoch cannot be made on the basis of existing data. This fact is especially true for batholiths of southern California and the Coast Range. The data do suggest, however, that the predominant Mesozoic granitic rocks in these areas are about 115 to 120 m.y. old but do not exclude the possibility that representatives of older and younger Mesozoic granitic rocks are present. The boundaries shown for rocks belonging to the five epochs are not to be considered the same as contacts that would be drawn on a geologic map. Detailed mapping in the field may change any of the traces, but the gross distribution cannot vary much from that indicated.

Granite emplacement during the Paleozoic in eastern Australia (Evernden and Richards, 1962) and during the Mesozoic in the Sierra Nevada covered comparable intervals of time. Spatial patterns of intrusion in the two areas, however, were different. Successive pulses of granitic rock were emplaced in a regular way from southwest to northeast in Australia with little intrusion of an earlier series by a later one. As shown on plate 1, vast volumes of younger granite in the Sierra Nevada now occupy terranes previously occupied by older plutons. The predominant area of Middle Triassic granites is to the east of the Sierra Nevada in the Mono Lake area. Rocks of the Early Jurassic epoch occur predominantly in the Inyo and White Mountains, but also occur in the eastern Sierra Nevada, the western foothill belt of the Sierra Nevada, and the Klamath Mountains in northern California. East of the Sierras, there is

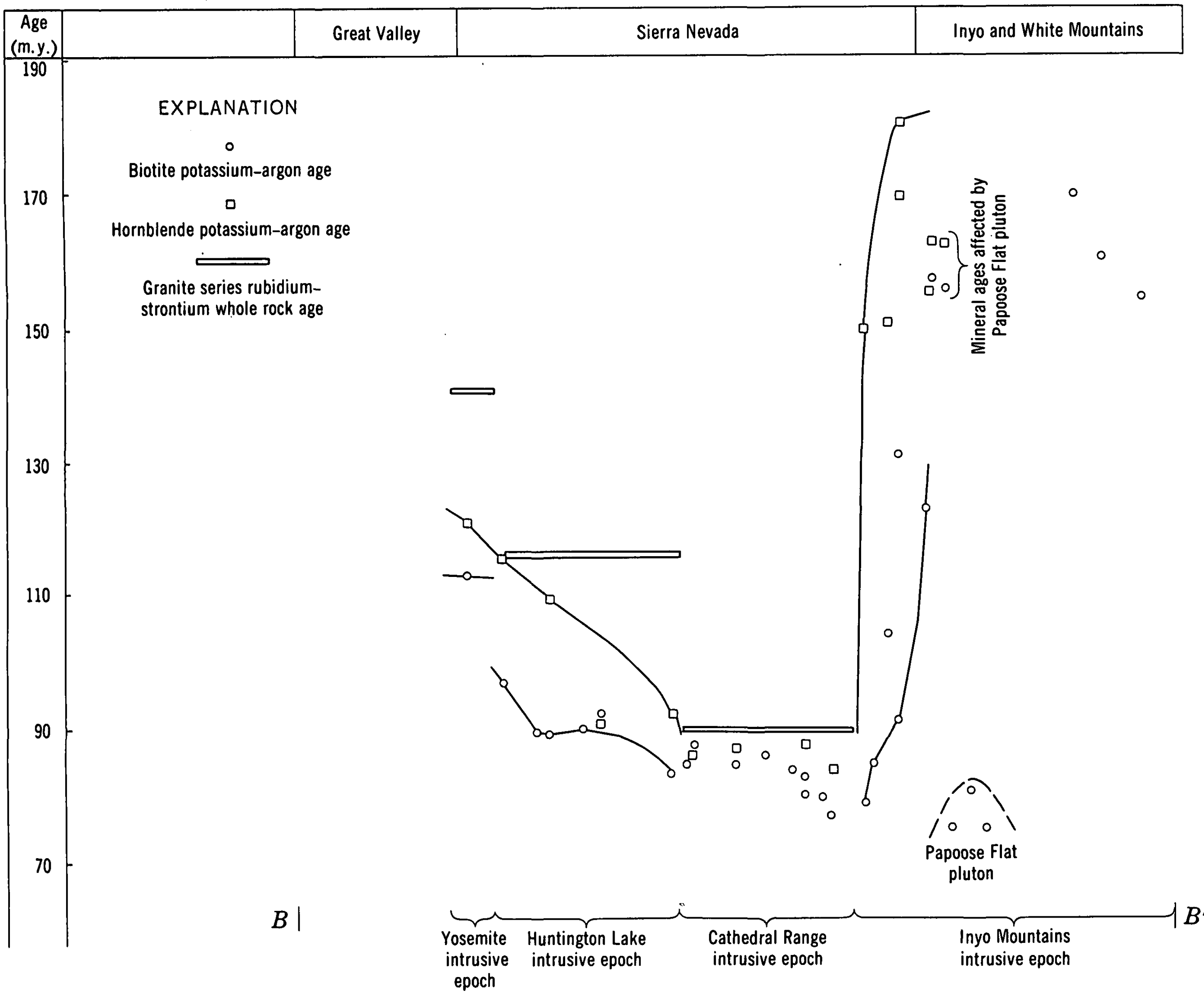

FIGURE 8.—Potassium-argon mineral ages and rubidium-strontium whole-rock ages for granitic rocks of the Inyo Mountains, Yosemite, Huntington Lake, and Cathedral Range intrusive epochs projected to a diagrammatic cross section of California. Location of cross section shown on plate 2.

not much replacement of rocks of one epoch by rocks of another; at a few places in the Inyo-White Mountain terrane, however, Late Cretaceous plutons crop out. The Mesozoic granitic rocks of southern California and those presently occurring in the Coast Ranges are predominantly of Early Cretaceous age, whereas the major mass of granites in the High Sierra are of Late Cretaceous age.

Present spatial distribution implies that rocks of all five intrusive epochs were emplaced in the region now defined by the crestal area of the Sierra Nevada from the latitude of Mono Lake southward and that massive replacement of rocks of each earlier intrusive epoch by invasion during succeeding epochs has taken place. The axis of emplacement shifted markedly in the Early and Late Cretaceous with associated replacement of the entire central portion of the Lower Jurassic batholith. It is probably significant that the deepest root of the Sierra Nevada is beneath this region.

UPLIFT OF PLUTONS OF THE TRANSVERSE AND COAST RANGES

If the age discordance shown by KA 1582 and KA 1582–HBD at the southern end of the Sierra Nevada is confirmed by additional dates, the pattern of biotite ages in that area may be interpreted as the result of uplift—as suggested by agreement of KA 1575–HBD (88 m.y.), KA 1575 (86 m.y.), KA 1582–HBD (86 m.y.) associated with disagreement of KA 1582–HBD (86 m.y.) and KA 1582 (74 m.y.) (table 5)—the hy-

359-835 O—69——4

pothesis being that the discordance is the result of erosion of these granitic rocks to great depth. The explanation of the decrease in topographic height of the mountain range south of Mount Whitney has always been a problem. An explanation based upon relative uplift would require either a flexure of the batholith or extensive faulting and downdropping of the southern end. Faulting is not supported by field data, and flexure is difficult to evaluate. A third possibility is that uplift was continuous in direction from north to south but that erosion rates were greater to the south; the postulation would be that the interplay of these two factors lead to a topographic culmination in the vicinity of Mount Whitney. Such an explanation might be indicated by a biotite-hornblende age discordance at Walker Pass, whereas an explanation based upon warping would not be substantiated by such discordance.

The potassium-argon mineral ages in the San Gabriel Mountains and in the Coast Range plutons are the youngest so far determined for Mesozoic granitic rocks in California. Biotite ages are as young as 61 m.y. (KA 1680) and hornblende ages as young as 70 m.y. (KA 1696–HBD). Age determinations by other techniques show that these granitic plutons are significantly older than indicated by the potassium-argon determinations, but geologic mapping indicates that the reduced mineral ages for these rocks are not attributable to intrusion of adjacent younger intrusions.

Another interpretation for the reduced mineral ages in the Coast Range plutons and in the San Gabriel plutons may be that the presently exposed levels of these rocks were once buried at depths where temperatures were sufficiently high to cause loss of accumulating argon from the minerals dated. However, some of the ages of biotite-hornblende pairs are concordant. Estimates from available diffusion data indicate that a temperature of about 650°C is required for hornblende to lose accumulating radiogenic argon at the same rate as biotite at 325°C. A temperature of 650°C would be attained at depths of approximately 20 to 26 km, depending upon the geothermal gradient. In the Santa Lucia Mountains, biotite and hornblende ages are concordant at 77 m.y. (Campanian) and the plutons are unconformably overlain by Campanian sedimentary rocks. To have the reduced ages due solely to high temperature resulting from deep burial of the presently exposed levels of these intrusions would require an uplift of 20 or more kilometers within a single geologic epoch. Since this rate of uplift seems excessive, the reduced ages are more likely due to a combination of burial, and abnormal heating and strain prior to the exposure of the plutons.

The effects of strain and physical disruption on the minerals dated has to be considered a cause for the reduced ages in the Coast Ranges, where most of the basement rocks are sheared. However, there is evidence that strain alone cannot be the cause of argon loss from biotite and hornblende in this terrane. First, specimens of Wheeler Crest Quartz Monzonite were collected from the mylonite zone of the eastern frontal scarp of the Sierra Nevada (specimens MT–3, MT–4, Kistler and others, 1965) with the intention of dating the time of faulting. Potassium-argon ages of biotite (69 m.y., MT–3; 79 m.y., MT–4) and of hornblende (96 m.y., MT–3; 99 m.y., MT–4) were grossly discordant in these rocks. The discordance indicated that the technique was useless for the purpose intended, that is, dating the time of faulting, but for the present discussion it is useful in indicating that strain results in discordant biotite-hornblende potassium-argon ages. The reduced potassium-argon ages are discordant in only one of the dated biotite hornblende pairs from the San Gabriel Mountains-Coast Range terrane. Second, the shearing in the Coast Range and San Gabriel Mountains basement rocks is probably due principally to Cenozoic tectonic events, but the concordant biotite-hornblende ages are all Late Cretaceous. Even though shearing of the Coast Range basement may have resulted in some loss of argon from minerals in the rocks, the two considerations made indicate that additional causes are necessary to explain the observed reduced concordant ages.

Geologic evidence indicates that the deepest crustal levels exposed in California are in the basement rocks which lie to the west of the San Andreas fault in the Coast Ranges and between the San Andreas fault and the San Gabriel fault in southern California. Metamorphic mineral assemblages of the Junipero Serra region of the Santa Lucia Range are of highest amphibolite facies and locally granulite facies (Compton, 1966). Precambrian gneisses and schists of high metamorphic grade are exposed between the San Andreas and San Gabriel faults in the San Gabriel Mountains. The Late Cretaceous mineral ages of Early Cretaceous and older Mesozoic plutons may reflect the time when these rocks were brought into crustal regions where they could cool to temperatures (about 300° C) that were compatible with equal retention of radiogenic argon in biotite and hornblende.

GRANITE EMPLACEMENT AND SEDIMENTATION ON THE CONTINENT

The relation between granite emplacement in the Sierra Nevada during the Cretaceous Period and the history of sedimentation in the Sacramento-San Joaquin Valley to the west is shown in figure 9. While constructing this figure, we discovered a previously published figure of similar type by Chuber (1962). The resulting figure 9 of this paper is then a modification

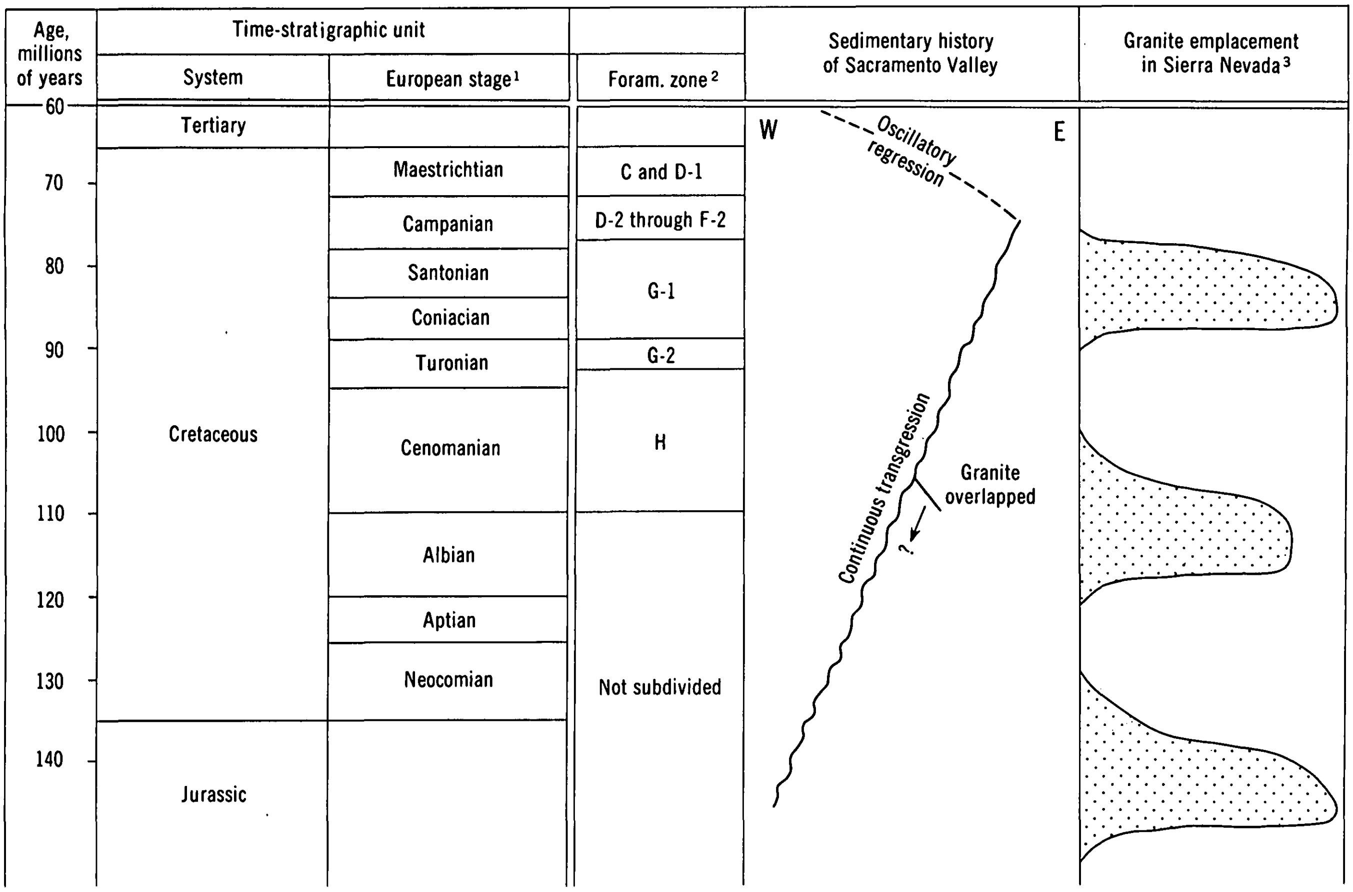

[1]Age of system and stage boundaries only approximate
[2]Foraminiferal zones of Goudkoff (1945)
[3]Varying width of stippled area is intended to show variation in volume of emplaced granite as a function of time. Diagrammatic only

FIGURE 9.—Relation of sedimentation in the Sacramento Valley to granite emplacement in the Sierra Nevada area (in part a modification and extension of Chuber, 1962).

and extension of his. Note on figure 9 the extent of overlap of presumably Jurassic granites that has occurred in the Great Valley (Smith, 1964; Hoffman, 1964; Callaway, 1964). Cenomanian sedimentary rocks are known to overlap granites in the Great Valley, and only deeper drilling farther west will determine the actual extent of such granitic rocks. Also, note that eastward transgression of the Cretaceous seas was continuous from the earliest Cretaceous to the time of the E-zone of Goudkoff (Forbes Shale of Edmondson, 1962), that is, throughout the entire period of emplacement, uplift, and erosion of Cretaceous granite a few tens of miles to the east. During all of this time, most of the Cretaceous sediment came from erosion of the Sierra Nevada (Chuber, 1962). Uppermost Cretaceous sediments presently occur in the subsurface approximately 10 miles east of Merced (Callaway, 1964). Most of the biotite in the Upper Cretaceous sediments on the west side of the Great Valley was derived from Cretaceous granites of the Sierra Nevada (Curtis and others, 1958). Only subsequent to the close of final granite emplacement did eastward transgression of the Cretaceous seas cease; oscillatory regression and eventual basin filling followed.

On a larger scale, the total time span of Mesozoic intrusion in California coincides with that of the transgression of Mesozoic epicontinental seas onto North America. This correspondence is revealed by comparing the ages of California granitic rocks with data on the transgressing epicontinental seas. From paleogeographic maps representing various stages of the Mesozoic and Cenozoic (Schuchert, 1955), Damon and Mauger (1966) plotted areas of marine deposition within the present boundaries of North America as percentages of continent inundated. We have reproduced their graph in figure 10. The curve clearly shows that the Mesozoic transgressive episode, which terminated in the Turonian stage of the Late Cretaceous, when 31 percent

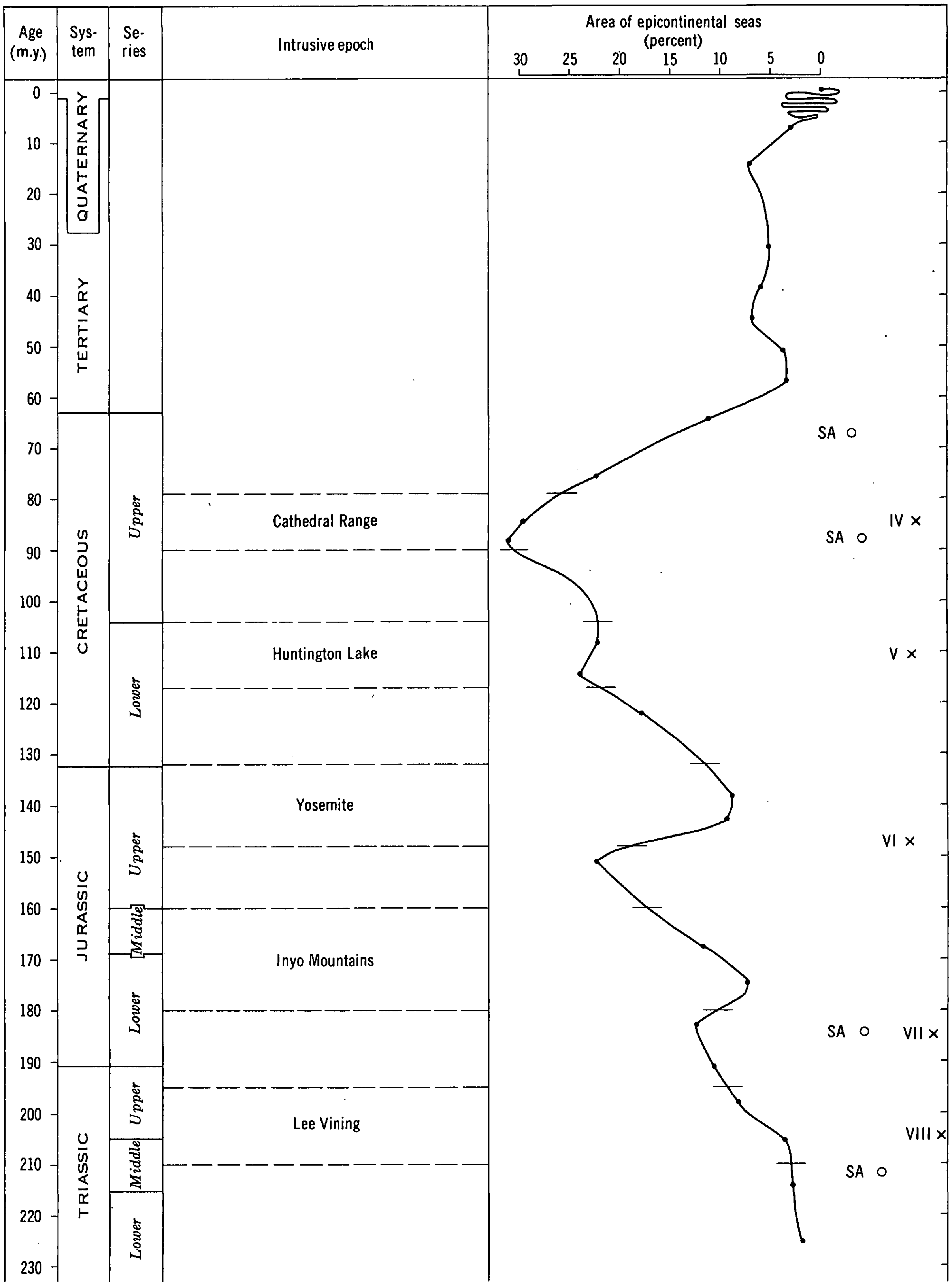

FIGURE 10.—(For explanation see facing page.)

of North America was inundated, had temporary but distinct reversals.

Damon and Mauger (1966) were concerned with the relationship between magmatism and orogeny in post-Turonian time. On the basis of available mica-potassium-argon ages of granitic rocks in the Great Basin, they showed two Cenozoic deformational and plutonic episodes to be coincident in time with the two reversals in the last 60 m.y. of their curve. They suggested then that transgression and regression of epicontinental seas reflected orogenic events and proposed that three other orogenies occurred within the time intervals represented by the three major withdrawals which occurred during the Mesozoic.

Our data require a refinement of this interpretation since the beginning of each Mesozoic plutonic episode is approximately coincident with a peak which marks the beginning of a temporary reversal of the general transgression curve. Also plotted in figure 10 are the intervals of time we have determined for each of the five epochs of granitic intrusion in the Mesozoic batholiths of California. The remarkable correlation between the presently known periods of temporary regression of the epicontinental seas and the periods of granite emplacement is obvious.

CORRESPONDENCE OF INTRUSIVE AND DEFORMATIONAL EVENTS IN THE SIERRA NEVADA

Immediately preceding, and in part contemporaneous with, each of the periods of voluminous magma intrusion, deformational events of regional extent occurred in California and western Nevada. The term pulse is used by us for each temporally related deformational and intrusive event. The five pulses are described as follows:

Early or Middle Triassic pulse (*Lee Vining intrusive epoch*).—Early or Middle Triassic deformation of regional extent in the Sierra Nevada folded layered Permian and older sedimentary and volcanic rocks in the Ritter Range pendant directly west of outcrops of granitic rocks intruded during the Lee Vining intrusive epoch (Kistler, 1966a).

Early and Middle Jurassic pulse (*Inyo Mountains intrusive epoch*).—Folding and thrusting that was well advanced before the end of deposition of the Early and Middle Jurassic Dunlap Formation occurred in the area immediately north of outcrops of Lower Jurassic granitic rocks of the Inyo-White Mountains batholith (Ferguson and Muller, 1949). Near its base, the Dunlap Formation contains fossils characteristic of the upper part of the Lower Jurassic or upper Lias of the European section.

Late Jurassic pulse (*Yosemite intrusive epoch*).—Folds in Upper Jurassic (Oxfordian and Kimmeridgian) metamorphosed sedimentary and volcanic rocks in the foothill belt of the Sierra Nevada are truncated by batholithic rocks of the Yosemite intrusive epoch. Folding and thrusting unquestionably preceded plutonic intrusion, and the two events may be considered component parts of a revolution according to Taliaferro (1942).

Early Cretaceous pulse (*Huntington Lake intrusive epoch*).—In the Santa Lucia Mountains of the California Coast Ranges, an unconformity between the Marmalejo Formation of Taliaferro (1944) of very early Cretaceous age, and the Jack Creek Formation of Taliaferro (1944) of early Late Cretaceous age, marks a late Early Cretaceous disturbance. In the Peninsular Ranges of California, a major unconformity occurs between marine strata of Late Cretaceous age and marine strata of Early Cretaceous and earliest Late Cretaceous ages (Jahns, 1954), the older rocks having been metamorphosed and then intruded by granitic rocks of the Huntington Lake intrusive epoch.

Late Cretaceous pulse (*Cathedral Range intrusive epoch*).—In the Jackson Mountains of northwestern Nevada, on line with the trend of granitic rocks of the Cathedral Range intrusive epoch exposed in the Sierra Nevada, Lower Cretaceous sedimentary rocks were folded and then eroded before deposition of the next younger rock unit of Late Cretaceous or early Tertiary age (Willden, 1958).

The record of the Cretaceous deformational events cannot be demonstrated in stratified rocks in roof pendants in most of the present physiographic Sierra Nevada (Kistler, 1966b) owing to previous intrusion of Jurassic and older granitic rocks. These granitic rocks were not susceptible to folding, as were the layered rocks folded on the flanks of the granite massifs. Local folding superimposed on Late Jurassic folds in Jurassic and Paleozoic sedimentary rocks in the foothill belt of the Sierra Nevada (Best, 1963) may be related to either of the two Cretaceous deformations.

The correlation of California tectonic and intrusive pulses with oscillations of the North American epicontinental seas implies that these pulses must have been significant throughout the entire Cordilleran region.

EXPLANATION OF FIGURE 10

Curve showing extent of expicontinental seas (after Damon and Mauger, 1966) during the Cenozoic and Mesozoic Eras (time scale after Harland and others, 1964). Circles marked SA represent oldest dates of South American intrusive rock intervals; the X's marked IV–VIII represent the oldest ages of the time intervals of Gabrielse and Reesor (1964) for intrusive rock series of British Columbia.

Age data from Mesozoic batholithic rocks in British Columbia, Canada, suggest a similar pattern. On the basis of about 50 mica potassium-argon ages, Gabrielse and Reesor (1964) separate five Mesozoic intrusive events which they designate with numbers VIII through IV. The oldest age determined for granitic rocks in each of these episodes is plotted next to its corresponding number on our figure 10. Stratigraphic evidence was used by Gabrielse and Reesor to show unconformities coincident with periods VIII, VII, and V. They state in their concluding remarks that "There appears to be a succession of pulsatory events at about 30 million year intervals, established in part by stratigraphy, and in part by potassium-argon determinations."

Potassium-argon dates by us from Mesozoic granitic rocks in the South American cordillera (Peru and Bolivia), although limited in coverage and number, indicate a similar periodic intrusive history. Of particular significance is the fact that the oldest Mesozoic batholithic rocks of this region are of Middle Triassic age (equivalent in age to the Lee Vining intrusive epoch). Other granitic rocks dated are equivalent in age to those emplaced in California during the Inyo Mountain and the Cathedral Range intrusive epochs. These data are shown on figure 10 and the locations of the samples of Middle Triassic age are given in table 5.

CONCLUSIONS

The emplacement of Mesozoic batholithic rocks in the North American cordillera was accomplished during five major pulses of deformation and intrusion (all five were not demonstrated for South America by our limited data). In addition, the patterns of deposition, in both western California and central North America, show that these regions were being lowered progressively by epeirogenic movement during the same period of time, culminating in the Turonian stage of the Late Cretaceous, when 31 percent of the present continental area was below sea level. A new geological term should be coined for such a profound and complex series of continent-wide (or hemisphere-wide) events as occurred in North America during this period of combined extensive foundering and massive intrusion and uplift. The term should be defined so as to stress the detailed correspondence in time of apparently secondary features of the phenomenon. It should be also stressed that, as the mass of intruded granite became greater, the inundations became greater. Only when massive emplacement of granite ceased, did emergence of the continent occur.

It is obvious that the fundamental explanation for mobilization of the magmas subsequently emplaced in eastern California cannot be found in localized downwarping of a deep sedimentary basin. Mechanisms much more profound than this must be found to explain the detailed correspondence of events here discussed. Present geological thought would probably attempt to find a driving mechanism for these events, either in complimentary phase changes or by horizontal convective transport of vast quantities of material. Both of these explanations actually depend upon an even more fundamental process, that is, a perturbation of uniform heat flow within the mantle of the earth. Both syntheses can, and probably will, be extensively developed.

REFERENCES CITED

Banks, P. O., and Silver, L. T., 1966, Evaluation of the decay constant of uranium 235 from lead isotope ratios: Jour. Geophys. Research, v. 71, no. 16, p. 4037–4046.

Bateman, P. C., 1961, Granitic formations in the east-central Sierra Nevada near Bishop, California: Geol. Soc. America Bull., v. 72, no. 10, p. 1521–1537.

Bateman, P. C., Clark, L. D., Huber, N. K., Moore, J. G., and Rinehart, C. D., 1963, The Sierra Nevada batholith—a synthesis of recent work across the central part: U.S. Geol. Survey Prof. Paper 414–D, 46 p.

Best, M. G., 1963, Petrology and structural analysis of metamorphic rocks in the southwestern Sierra Nevada foothills, California: California Univ. Pubs. Geol. Sci., v. 42, no. 3, p. 111–158.

Broderson, R. A., 1962, The petrology, structure, and age relationships, Cathedral Peak porphyritic quartz monzonite, central Sierra Nevada, California: California Univ. (Berkeley), Ph. D. thesis, 287 p.

Callaway, D. C., 1964, Distribution of uppermost Cretaceous sands in the Sacramento-northern San Joaquin Basin of California: San Joaquin Geol. Soc. Selected Papers, v. 2, p. 5–18.

Calkins, F. C., 1930, The granitic rocks of the Yosemite region, *in* Matthes, F. E., Geologic history of the Yosemite Valley: U.S. Geol. Survey Prof. Paper 160, p. 120–129.

Christensen, M. N., 1959, Geologic structure of the Mineral King area, California: California Univ. (Berkeley), Ph. D. thesis.

Chuber, Stewart, 1962, Late Mesozoic stratigraphy of the Sacramento Valley: San Joaquin Geol. Soc. Selected Papers, v. 1, p. 3–16.

Compton, R. R., 1966, Granitic and metamorphic rocks of the Salinian block, California Coast Ranges: California Div. Mines and Geology Bull. 190, p. 277–287.

Curtis, G. H., 1951, The geology of the Topaz Lake quadrangle and the eastern half of the Ebbetts Pass, California quadrangle: California Univ. (Berkeley), Ph. D. thesis, 316 p.

Curtis, G. H., Evernden, J. F., and Lipson, J., 1958, Age determination of some granitic rocks in California by the potassium-argon method: California Div. Mines Spec. Rept. 54, 16 p.

Damon, P. E., and Mauger, R. L., 1966, Epeirogeny-orogeny viewed from the Basin and Range province: Soc. Mining Engineer Trans., v. 235, no. 1, p. 99–112.

Davis, G. A., 1961, Metamorphic and igneous geology of pre-Cretaceous rocks, Coffee Creek area, northern Trinity Alps, Klamath Mountains, California: California Univ. (Berkeley), Ph. D. thesis.

Edmondson, W. F., 1962, Stratigraphic relations of Upper Cretaceous rocks in Great Valley, California: San Joaquin Geol. Soc. Selected Papers, v. 1, p. 17–26.

Ellis, A. J., and Fyfe, W. S., 1956, A note on the calcite-wollastonite equilibrium: Am. Mineralogist, v. 41, nos. 9–10, p. 805–807.

Evernden, J. F., and Curtis, G. H., 1965, The potassium-argon dating of late Cenozoic rocks in East Africa and Italy: Current Anthropology, v. 6, p. 343–385.

Evernden, J. F., Curtis, G. H., Kistler, R. W., and Obradovich, J. D., 1960, Argon diffusion in glauconite, microcline, sanidine, leucite, and phlogopite: Am. Jour. Sci., v. 258, no. 8, p. 583–604.

Evernden, J. F., and James, G. T., 1964, Potassium-argon dates and the Tertiary floras of North America: Am. Jour. Sci., v. 262, no. 8, p. 945–974.

Evernden, J. F., and Richards, J. R., 1962, Potassium-argon ages in eastern Australia: Geol. Soc. Australia Jour., v. 9, pt. 1, p. 1–50.

Evernden, J. F., Savage, D. E., Curtis, G. H., and James, G. T., 1964, Potassium-argon dates and the Cenozoic mammalian chronology of North America: Am. Jour. Sci., v. 262, no. 2, p. 145–198.

Ferguson, H. G., and Muller, S. W, 1949, Structural geology of the Hawthorne and Tonopah quadrangles, Nevada.: U.S. Geol. Survey Prof. Paper 216, 55 p.

Fyfe, W. S., Turner, F. J., and Verhoogen, John, 1958, Metamorphic reactions and metamorphic facies: Geol. Soc. America Mem. 73, 259 p.

Gabrielse, H., and Reesor, J. E., 1964, Geochronology of plutonic rocks in two areas of the Canadian Cordillera, *in* Osborne, F. F., ed., Geochronology in Canada: Royal Soc. Canada Spec. Pub. 8, p. 96–128.

Goudkoff, P. P., 1945, Stratigraphic relations of Upper Cretaceous in Great Valley, California: Am. Assoc. Petroleum Geologists Bull., v. 29, no. 7, p. 956–1007.

Gromme, C. S., 1963, Remanent magnetization of igneous rocks from the Franciscan and Lovejoy Formations, northern California: California Univ. (Berkeley), Ph. D. thesis, 226 p.

Hall, W. E., and MacKevett, E. M., Jr., 1962, Geology and ore deposits of the Darwin quadrangle, Inyo County, California: U.S. Geol. Survey Prof. Paper 368, 87 p.

Hamilton, W. B., 1956, Geology of the Huntington Lake area, Fresno County, California: California Div. Mines Spec. Rept. 46, 25 p.

Harland, W. B., Smith, A. C., and Wilcock, Bruce, eds., 1964, The Phanerozoic time-scale—A symposium dedicated to Professor Arthur Holmes: Geol. Soc. London Quart. Jour., Supp., v. 120s, 458 p.

Hart, S. R., 1964, The petrology and isotopic-mineral age relations of a contact zone in the Front Range, Colorado: Jour. Geology, v. 72, no. 5, p. 493–525.

Hay, E. A., 1963, Age and relationship of the Gold Hill Pluton, Cholame Valley, California, *in* Am. Assoc. Petroleum Geologists Soc. Econ. Paleontologists and Mineralogists, Pacific Section, Guidebook to the geology of Salinas Valley and the San Andreas fault: p. 113–115.

Hoffman, R. D., 1964, Geology of the northern San Joaquin Valley [California]: San Joaquin Geol. Soc. Selected Papers, v. 2, p. 30–45.

Holdaway, M. J., 1963, Petrology and structure of metamorphic and igneous rocks of parts of northern Coffee Creek and Cecilville quadrangle, Klamath Mountains, California: California Univ. (Berkeley), Ph. D. thesis, 202 p.

Holm, J. L., and Kleppa, O. J., 1966, The thermodynamic properties of the aluminum silicates: Am. Mineralogist, v. 51, nos. 11–12, p. 1608–1622.

Hurley, P. M., Bateman, P. C., Fairbairn, H. W., and Pinson, W. E., Jr., 1965, Investigation of the Initial Sr^{87}/Sr^{86} ratios in the Sierra Nevada plutonic province: Geol. Soc. America Bull., v. 76, no. 2, p. 165–174.

Jaffe, H. W., Gottfried, David, Waring, C. L., and Worthing, H. W., 1959, Lead-alpha age determinations of accessory minerals of igneous rocks (1953-1957): U.S. Geol. Survey Bull. 1097–B p. 65–148.

Jahns, R. H., 1954, Geology of the Peninsular Range province, southern California and Baja California [Mexico]: [pt.] 3 *in* Chap. 2 *of* Jahns, R. H., ed., Geology of southern California: California Div. Mines and Geology Bull. 170, p. 29–52.

Jenkins, S. F., 1961, A structural study of a portion of the Kernville Series (?Jurassic; California): California Univ. (Berkeley), M.A. thesis.

Kistler, R. W., 1966a, Geologic map of the Mono Craters quadrangle, Mono and Tuolumne Counties, California: U.S. Geol. Survey Geol. Quad. Map GQ–462, scale 1: 62,500.

———1966b, Structure and metamorphism in the Mono Craters Quadrangle Sierra Nevada, California: U.S. Geol. Survey Bull. 1221–E, 53 p.

———1968, Potassium-argon ages of volcanic rocks in Nye and Esmeralda Counties, Nevada: Geol. Sec. America Mem. 110. p. 251–262.

Kistler, R. W., Bateman, P. C., and Brannock, W. W., 1965, Isotopic ages of minerals from granitic rocks of the central Sierra Nevada and Inyo Mountains, California: Geol. Soc. America Bull., v. 76, no. 2, p. 155–164.

Kistler, R. W., and Dodge, F. C. W., 1966, Potassium-argon ages of coexisting minerals from pyroxene-bearing granitic rocks in the Sierra Nevada, California: Jour. Geophys. Research, v. 71, no. 8, p. 2157–2161.

Krauskopf, K. B., 1953, Tungsten deposits of Madera, Fresno, and Tulare Counties, California: California Div. Mines Spec. Rept. 35, 83 p.

Larsen, E. S., Jr., 1948, Batholith and associated rocks of Corona, Elsinore, and San Luis Rey quadrangle, southern California: Geol. Soc. America Mem. 29, 182 p.

Macdonald, G. A., 1941, Geology of the western Sierra Nevada between the Kings and San Joaquin River, California: California Univ. Pubs. Geol. Sci., v. 26, no. 2, 215–286.

Mayo, E. B., 1941, Deformation in the interval Mt. Lyell-Mt. Whitney, California: Geol. Soc. America Bull., v. 52, no. 7, p. 1001–1084.

McKee, E. H., 1962, The stratigraphy and structure of a portion of the Magruder Mountain-Soldier Pass quadrangles, California-Nevada: California Univ. (Berkeley), Ph. D. thesis, 108 p.

McKee, E. H., and Nash, D. B., 1967, Potassium-argon ages of granitic rocks in the Inyo Batholith, east-central California: Geol. Soc. America Bull., v. 78, p. 669–680.

McKee, E. H., and Nelson, C. A., 1967, Geologic map of the Soldier Pass quadrangle, California and Nevada: U.S. Geol. Survey Geol. Quad. Map GQ–654, scale 1: 62,500.

Miller, W. J., 1931, Geologic sections across the southern Sierra Nevada of California: California Univ. Pubs. Geol. Sci., v. 20, no. 9, p. 331–360.

Miller, W. J., and Webb, R. W., 1940, Descriptive geology of the Kernville quadrangle, California: California Jour. Mines and Geology, v. 36, no. 4, p. 343–378.

Parker, R. B., 1961, Petrology and structural geometry of pre-granitic rocks in the Sierra Nevada, Alpine County, California: Geol. Soc. America Bull., v. 72, no. 12, p. 1789–1806.

Rama, S. N. I., Hart, S. R., and Roedder, E., 1965, Excess radiogenic argon in fluid inclusions: Jour. Geophys. Research, v. 70, p. 509–511.

Romey, W. D., 1962, Geology of a part of the Etna quadrangle, Siskiyou County, California: California Univ. (Berkeley), Ph. D. thesis.

Ross, D. C., 1965, Geology of the Independence quadrangle, Inyo County, California: U.S. Geol. Survey Bull. 1181–O, 64 p.

Schuchert, Charles, 1955, Atlas of paleogeographic maps of North America: New York, John Wiley & Sons, Inc.

Sherlock, D. G., and Hamilton, W. B., 1958, Geology of the north half of the Mount Abbot quadrangle, Sierra Nevada, California: Geol. Soc. America Bull., v. 69, no. 10, p. 1245–1267.

Slemmons, D. B., 1953, Geology of the Sonora Pass Region: California Univ. (Berkeley), Ph. D. thesis, 201 p.

Smith, M. B., 1964, Map showing distribution and configuration of basement rocks in California: U.S. Geol. Survey Oil and Gas Inv. Map OM–215, scale 1:500,000.

Taliaferro, N. L., 1942, Geologic history and correlation of the Jurassic of southwestern Oregon and California: Geol. Soc. America Bull., v. 53, no. 1, p. 71–112.

———1944, Cretaceous and Paleocene of Santa Lucia Range, California: Am. Assoc. Petroleum Geologists Bull., v. 28, no. 4, p. 449–521.

Weill, D. F., 1966, Stability relations in the Al_2O_3-SiO_2 system calculated from solubilities in the Al_2O_3-SiO_2-Na_3AlF_6 system: Geochim. et Cosmochim. Acta, v. 30, no. 2, p. 223–237.

Willden, C. R., 1958, Cretaceous and Tertiary orogeny in Jackson Mountains, Humboldt County, Nevada: Am. Assoc. Petroleum Geologists Bull., v. 42, no. 10, p. 2378–2398.

TABLES 5 and 6

TABLE 5.—*Potassium-argon analyses and location of sample localities*

[The following ages (also shown on pl. 2) for the location numbers given were taken from previously published data: 155–166 (Curtis and others, 1958); 167–168 (Kistler and Dodge, 1966); 169–206 (localities 2–39 respectively of Kistler and others, 1965); 207–208 (Hall and MacKevett, 1962); 250–251 (Compton, 1966). Constants: $\lambda_\beta=4.72\times10^{-10}$ year^{-1}; $\lambda_\epsilon=0.584\times10^{-10}$ year^{-1}; 1.19×10^{-4} atoms K^{40}/atoms K]

Location No. (pl. 1)	KA No.	Latitude (N.)	Longitude (W.)	Elevation (ft)	Picked (P) or unpicked (U)	Mineral	Size (standard mesh)	Weight (grams)	K (wt percent)	Ar_{at}^{40} (percent)	Age (10^6 yr)	$\delta_{(x-y)}$ (percent)
62	67-64	37°41′43″	119°43′29″		U	Biotite		0.398	7.210	9	93.3	0.1
63	71-64	37°42′35″	119°43′16″		U	do		.332	7.516	9	92.9	.3
64	72-64	37°43′25″	119°42′49″		U	do	16/35	.438	7.531	11	90.0	.1
21	131-64	38°37′32″	119°32′27″	5,200	P	do		.333	7.709	11	81.9	.0
65	579	37°22′22″	117°58′38″		U	do		.555	5.476	30	170.0	1.3
66	804	37°01′21″	118°06′36″		U	do		.655	5.663	40	77.9	1.3
121	820	35°49′46″	118°28′50″		U	do		1.187	6.66	14	84.7	2.0
122	822	35°45′55″	118°24′40″		U	do		1.756	6.58	47	48.8	.1
4	828	40°59′39″	122°55′06″		U	do		.728	5.90	10	130	.5
67	840	37°23′08″	117°43′47″		U	do		.767	5.10	23	155	1.9
123	842	35°49′50″	120°21′10″		U	Hornblende			.108	82	143	.9
68	902	37°25′36″	117°53′49″		U	Biotite		.360	5.608	16	162	.0
1	955	41°21′13″	122°58′10″		U	do	28/60	3.207	5.184	9	143.5	1.4
2	956	41°18′38″	122°58′24″		U	do	16/28	3.071	6.513	4	141	1.8
3	957	41°09′37″	122°58′06″		U	do	16/28	2.469	6.364	6	130	1.1
10	1432	39°53′52″	121°21′16″		P	do	8/10	.412	7.607	6	128	.6
	1433	39°53′52″	121°21′16″		P	Hornblende	10/16	.627	.646	17	142	.4
11	1436	39°58′15″	121°16′37″		P	Biotite	16/35	.350	7.031	10	132	.3
	1437	39°58′15″	121°16′37″		P	Hornblende	28/60	1.167	.550	50	136	.0
12	1438	39°45′35″	121°18′34″		P	Biotite	16/28	.318	7.335	7	126	.1
	1439	39°45′35″	121°18′34″		P	Hornblende	16/28	1.319	.582	24	131	.3
13	1440	39°49′44″	121°24′18″		P	Biotite	8/10	.351	7.485	6	129	.6
	1441	39°49′44″	121°24′18″		P	Hornblende	16/28	1.372	.577	24	132	.2
14	1442	39°57′57″	121°16′37″		P	do	28/48	1.158	.452	32	143	.5
	1449	39°57′57″	121°16′37″		P	do	35/48	2.451	.451	14	142	.6
167	1495	(Kistler FD-13)			P	Biotite	35/80	.285	7.858	19	87.4	.1
5	1501	40°34′39″	120°44′14″	5,600	P	do	16/28	.330	7.142	7	123	.2
6	1502	40°34′43″	120°43′02″	5,350	P	do	16/28	.399	7.284	3	121	.7
	1502-HBD				P	Hornblende	100/200	1.995	3.374	4	121	.1
7	1503	40°15′44″	120°31′38″	5,400	P	Biotite	16/28	.440	7.733	8	97.4	.3
8	1504	40°14′39″	121°31′00″	6,030	P	do	10/16	.352	7.302	7	99.9	.0
9	1506	40°07′04″	120°28′40″	5,515	P	do	60/100	.294	6.893	14	101	.3
	1506-HBD				P	Hornblende	100/150	2.907	3.017	8	102	1.0
20	1508	39°47′31″	120°06′25″	5,040	P	Biotite	16/28	.354	7.821	7	86.8	.1
	1508-R				P	do	16/28	.367	7.821	8	86.6	
	1508-B				P	do	16/28	.391	7.549	6	88.9	.4
	1508-B-R				P	do	16/28	.394	7.549	7	89.0	
15	1509	39°52′07″	120°24′07″	5,613	P	do	16/28	.343	7.474	4	105	.5
	1509-HBD				P	Hornblende	28/60	1.707	.672	7	105	.3
15a	1510	39°36′38″	120°29′37″	7,000	P	Biotite	10/16	.383	5.814	56	99.0	.7
16	1511	39°37′14″	120°28′30″	6,400	P	do	16/28	.353	7.438	9	97.2	.1
	1511-10/16				U	do	10/16	.486	6.699	9	97.5	.7
	1511-16/28				U	do	16/28	.365	6.176	8	98.5	.1
	1511-35/48				U	do	35/48	.306	6.799	9	101	.7
	1511-100/150				U	do	100/150	.420	7.093	8	101	.1
	1511-HBD				P	Hornblende	35/60	.853	.876	15	125	.5
17	1512	39°19′06″	120°18′54″	6,680	P	Biotite	10/16	.402	7.429	11	96.7	.4
	1512-HBD				P	Hornblende	28/60	1.447	.666	27	97.8	.5
	1512-PL				P	Plagioclase	28/60	2.209	.299	35	92.5	.1
	1512-KF				P	K-feldspar	60/100	.448	11.54	3	100.1	.0
	1512-QTZ				P	Quartz	28/60	3.507	.028	84	109	
22	1514	38°51′59″	120°04′40″	7,550	P	Biotite	16/28	.402	7.224	5	87.8	.5
	1514-HBD				P	Hornblende	28/100	.492	.840	27	91.4	.1
23	1516	38°58′37″	119°53′15″	7,360	P	Biotite	16/28	.363	7.557	20	86.1	.1
	1516-HBD				P	Hornblende	28/60	2.107	.937	33	89.9	.6
24	1517	38°57′52″	119°51′00″	5,200	P	Biotite	10/16	.392	7.359	9	83.5	.5
25	1518	38°47′07″	119°52′50″	7,500	P	do	10/16	.347	7.571	14	87.1	.3
	1518-R				P	do	10/16	.361	7.571	15	87.4	.3
26	1519	38°36′54″	120°13′21″	7,250	P	do	16/28	.327	7.445	10	91.7	.3
	1519-HBD				P	Hornblende	60/100	.516	.823	10	99.6	.7
27	1520	38°42′20″	120°05′53″	7,720	P	Biotite	16/28	.349	7.740	4	94.3	.5
28	1521	38°41′41″	119°44′15″	8,560	P	do	16/28	.493	7.519	4	88.7	.2
29	1523	38°29″16′	119°59′03″	7,500	P	do	10/16	.388	7.632	6	89.4	.1
30	1524	38°34′56″	119°47′55″	7,600	P	do	16/28	.296	6.656	7	81.8	.3
38	1525	37°49′29″	119°30′05″	8,800	P	do	10/16	.398	7.501	10	82.1	.7
69	1526	37°51′00″	119°26′45″	8,800	P	do	10/16	.353	7.778	8	82.4	.1
	1526-R				P	do	10/16	.472	7.778	7	83.7	.1
70	1527	37°51′08″	119°26′38″	8,800	P	do	10/16	.349	7.602	15	81.9	.0
	1527-8/10				U	do	8/10	.419	7.315	10	80.2	.8
	1527-10/16				U	do	10/16	.477	7.166	7	80.0	.4
	1527-16/28				U	do	16/28	.375	6.880	8	82.0	.3
	1527-35/48				U	do	35/48	.419	4.344	8	85.7	.1
	1527-48/60				U	do	48/60	.353	3.171	10	86.9	1.5
	1527-60/100				U	do	60/100	.354	2.825	12	84.7	.1
	1527-100/150				U	do	100/150	.674	1.630	29	90.8	.6
71	1528	37°52′34″	119°23′38″	8,800	P	do	16/28	.373	6.845	12	84.6	.7
72	1530	37°47′42″	119°23′42″	9,000	P	do	10/16	.395	7.053	12	83.7	.2
73	1531	37°45′26″	119°23′42″	9,000	P	do	16/28	.350	7.443	10	83.6	.3
74	1532	37°51′13″	119°17′50″	8,800	P	do	10/16	.365	7.581	7	83.2	.4
75	1533	37°51′44″	119°17′49″	8,800	P	do	16/28	.334	7.545	11	82.5	.4
	1533-HBD				P	Hornblende	28/60	1.678	.670	39	84.3	.0
	1533-PL				P	Plagioclase	60/100	1.993	.310	61	70.3	3.0
	1533-KF				P	K-feldspar	28/35	.400	11.95	2	73.5	.5
	1533-QTZ				P	Quartz	28/60	5.220	.025	78	88.9	
31	1534	38°35′05″	119°41′42″	6,640	P	Biotite	16/28	.372	6,272	8	82.1	.2
	1535	38°21′00″	119°39′08″	10,200	P	do	16/28	.371	7.444	12	82.8	.7
32	1536	38°25′45″	119°44′50″	7,450	P	do	16/28	.438	7.286	7	81.7	.0
33	1537	38°20′27″	119°49′27″	5,831	P	do	16/28	.367	7.247	7	84.3	.8
34	1538	38°21′49″	119°52′13″	5,520	P	do	8/10	.343	7.591	5	83.0	.1
	1538-R				P	do	8/10	.407	7.591	8	83.6	.1
	1538-HBD				P	Hornblende	28/60	2.030	.585	23	84.2	.2
35	1539	38°19′35″	119°55′07″	6,410	P	Biotite	10/16	.474	7.834	8	87.0	.2
	1539-HBD				P	Hornblende	28/35	2.025	.821	13	90.1	.6

TABLE 5.—*Potassium-argon analyses and location of sample localities*—Continued

Location No. (pl. 1)	KA No.	Latitude (N.)	Longitude (W.)	Elevation (ft)	Picked (P) or unpicked (U)	Mineral	Size (standard mesh)	Weight (grams)	K (wt percent)	Ar_{at}^{40} (percent)	Age (10^6 yr)	$\delta_{(x-y)}$ (percent)
36	1540	38°17′05″	119°57′56″	6,080	P	Biotite	10/16	.352	7.767	7	88.7	.0
	1540-HBD				P	Hornblende	60/100	1.980	.839	33	96.7	.6
37	1541	38°11′59″	120°00′07″	5,250	P	Biotite	10/16	.349	7.705	6	94.4	.7
	1541-R				P	do	10/16	.335	7.705	7	94.0	.7
	1541-HBD				P	Hornblende	28/60	2.309	.736	14	97.8	.9
	1541-PL				P	Plagioclase	28/60	1.926	.233	42	90.7	.1
	1541-KF				P	K-feldspar	28/35	.405	12.25	3	83.5	.5
	1541-QTZ				P	Quartz	28/60	2.776	.019	92	108	----------
38	1542	38°22′51″	119°52′14″	7,650	P	Biotite	10/16	.487	7.713	7	84.8	.5
39	1543	38°22′54″	119°52′07″	7,600	P	do	10/16	.315	7.676	6	82.9	.3
	1545	38°17′19″	119°43′06″	7,360	P	do	16/28	.340	7.369	8	82.7	.4
40	1546	38°24′58″	119°50′00″	7,560	P	do	8/10	.349	7.330	5	84.2	.3
41	1547	38°25′05″	119°49′47″	7,400	P	do	10/16	.370	7.347	4	85.6	.4
42	1548	38°26′45″	119°40′12″	7,600	P	do	35/48	.213	6.994	9	81.5	.1
	1548-R				P	do	35/48	.182	6.994	6	81.8	.1
43	1549	38°25′31″	119°42′17″	7,500	P	do	16/28	.453	7.102	8	81.1	.2
44	1550	38°23′56″	119°36′26″	10,040	P	do	16/28	.342	6.682	9	79.5	.2
76	1551	37°27′15″	118°50′19″	11,500	P	do	16/28	.431	7.009	6	79.1	.2
77	1552	37°26′06″	118°50′06″	9,000	P	do	16/28	.397	6.792	10	78.1	.0
78	1553	37°25′08″	118°46′04″	11,500	P	do	10/16	.464	7.142	15	78.8	.0
	1553-HBD				P	Hornblende	60/100	.800	.719	42	77.4	.4
79	1554	37°02′38″	118°31′41″	11,500	P	Biotite	16/28	.328	7.212	7	80.1	.1
80	1555	37°03′11″	118°34′46″	8,080	P	do	16/28	.379	7.067	8	80.1	.3
94	1556	36°46′27″	118°22′50″	11,500	P	do	16/28	.368	7.451	11	82.1	.4
81	1559	37°39′15″	119°05′27″	9,247	P	do	16/28	.354	7.621	12	78.7	.1
82	1560	37°39′10″	119°05′27″	9,000	P	do	28/35	.377	7.973	12	77.4	.4
83	1561	37°20′27″	118°45′58″	11,500	P	do	16/28	.335	6.845	8	79.6	.8
126	1562	35°43′58″	118°23′28″	2,800	P	do	16/28	.366	7.177	8	86.6	.0
127	1563	35°59′13″	118°29′47″	4,000	P	do	28/35	.387	7.486	7	89.7	.1
95	1564	36°03′15″	118°32′23″	6,200	P	do	10/16	.349	7.528	16	88.5	.2
	1564-HBD				P	Hornblende	28/60	1.916	1.070	11	95.6	.9
	1564-PL				P	Plagioclase	28/60	2.154	.277	49	72.6	.8
	1564-KF				P	K-feldspar	35/48	.495	11.69	2	87.5	.3
	1564-QTZ				P	Quartz	28/60	3.323	.014	92	57.9	----------
96	1565	36°07′33″	118°33′22″	6,730	P	Biotite	16/28	.351	7.472	6	87.5	.3
97	1566	36°09′03″	118°34′57″	5,800	P	do	16/28	.317	7.618	9	87.8	.0
	1566-R				P	do	16/28	.354	7.618	10	88.2	.0
	1566-B				P	do	16/28	.309	7.548	7	88.7	.5
	1566-B-R				P	do	16/28	.371	7.548	9	88.2	.5
98	1568	36°09′12″	118°14′39″	2,000	P	do	16/28	.388	7.522	7	91.5	.0
	1568-HBD				P	Hornblende	16/28	1.033	.877	17	96.3	.5
124	1569	35°44′36″	118°54′12″	1,100	P	Biotite	10/16	.353	7.971	5	102	.1
	1569-HBD				P	Hornblende	28/60	1.714	.590	24	108	.3
	1569-PL				P	Plagioclase	60/100	2.015	.774	20	102	2.0
	1569-KF				P	K-feldspar	28/60	.265	9.253	6	100	.5
	1569-QTZ				P	Quartz	28/60	2.619	.041	91	58	----------
125	1570	35°42′57″	118°48′58″	1,925	P	Biotite	8/10	.427	7.829	9	98.0	.1
	1570-HBD				P	Hornblende	28/60	1.948	.493	18	102	.7
128	1571	35°42′21″	118°45′06″	3,200	P	Biotite	16/28	.348	7.527	10	98.2	.5
129	1572	35°44′17″	118°38′56″	4,000	P	do	10/16	.362	7.556	10	92.3	.0
130	1573	35°44′51″	118°35′14″	4,875	P	do	16/28	.332	7.657	11	90.6	.1
131	1574	35°44′00″	118°32′52″	5,780	P	do	16/28	.356	7.273	10	87.7	.1
132	1575	35°41′38″	118°29′51″	3,750	P	do	16/28	.360	7.127	15	85.5	.0
	1575-HBD				P	Hornblende	28/60	1.364	1.066	12	87.7	.6
133	1576	35°39′24″	118°29′06″	2,700	P	Biotite	16/28	.403	7.392	9	87.0	.3
134	1577	35°39′05″	118°24′54″	2,850	P	do	16/28	.339	7.042	13	85.1	.3
135	1578	35°39′24″	118°19′17″	2,625	P	do	10/16	.367	7.692	10	79.2	.2
136	1579	35°41′48″	118°12′50″	2,800	P	do	35/48	.389	7.335	9	78.7	.4
137	1580	35°43′46″	118°10′00″	2,900	P	do	48/60	.277	7.393	13	78.2	.6
138	1581	35°45′01″	118°06′19″	3,450	P	do	35/48	.390	6.884	20	66.1	.4
139	1582	35°41′45″	118°03′18″	4,410	P	do	16/28	.385	7.620	21	74.0	.9
	1582-HBD				P	Hornblende	16/28	2.038	.905	17	86.2	.5
99	1583	36°35′44″	118°06′10″	4,370	P	Biotite	10/16	.440	7.583	13	81.8	.5
100	1584	36°35′10″	118°14′30″	8,480	P	do	16/28	.370	7.373	11	79.1	.2
	1584-HBD				P	Hornblende	60/150	1.914	.620	37	80.0	.4
101	1585	36°17′10″	118°08′20″	9,500	P	Biotite	16/28	.479	7.047	6	79.8	.8
102	1586	36°25′04″	118°16′23″	9,680	P	do	10/16	.360	7.632	10	80.5	.4
103	1587	36°35′04″	118°24′09″	9,280	P	do	10/16	.393	7.623	4	78.4	.6
	1587-R				P	do	10/16	.338	7.623	10	78.4	.6
	1587-HBD				P	Hornblende	60/100	1.694	.508	14	84.0	.6
104	1588	36°34′25″	118°19′06″	11,530	P	Biotite	16/28	.396	6.944	7	81.8	.2
105	1589	36°39′08″	118°22′02″	11,500	P	do	16/28	.350	7.170	16	79.6	.5
106	1590	36°33′34″	118°17′27″	13,777	P	do	16/28	.354	7.391	11	81.9	.6
	1590-R				P	do	16/28	.227	7.391	16	81.5	.6
107	1591	36°34′02″	118°16′05″	11,600	P	do	16/28	.335	6.932	7	79.3	.8
108	1592	36°35′34″	118°13′18″	7,680	P	do	10/16	.397	7.725	8	80.1	.1
	1592-HBD				P	Hornblende	28/60	2.069	.459	20	81.5	.6
	1593	37°50′52″	119°24′17″	10,900	P	Biotite	16/28	.336	7.100	7	83.4	.9
84	1594	37°52′41″	119°20′38″	8,700	P	do	16/28	.410	7.120	9	82.4	.1
45	1595	38°07′24″	119°25′39″	11,000	P	do	16/28	.441	7.296	10	81.0	.8
46	1596	38°07′32″	119°26′08″	9,200	P	do	28/48	.475	6.979	9	81.4	.1
47	1597	38°08′54″	119°25′36″	7,950	P	do	16/28	.402	7.435	5	80.2	.1
48	1598	38°08′54″	119°23′19″	7,300	P	do	16/28	.368	7.598	9	80.1	.1
49	1599	38°10′16″	119°31′02″	9,000	P	do	16/28	.437	7.208	10	81.4	.5
85	1600	37°09′11″	118°42′51″	11,500	P	do	28/35	.361	6.464	11	83.8	.3
86	1601	37°11′28″	119°40′00″	12,880	P	do	10/16	.364	7.276	9	82.5	.5
	1601-HBD				P	Hornblende	28/60	2.065	.770	12	88.4	.8
109	1602	36°27′05″	118°47′48″	2,400	P	Biotite	10/16	.383	7.626	6	91.7	.1
110	1603	36°26′56″	118°46′24″	3,050	P	do	10/16	.354	7.716	8	92.6	.1
111	1604	36°25′54″	118°45′18″	3,900	P	do	16/28	.367	7.193	25	82.7	.3
112	1605	36°26′20″	118°44′22″	4,050	P	do	10/16	.367	7.531	15	87.4	.2
	1605-HBD				P	Hornblende	28/60	1.338	.888	20	90.1	.2
	1605-PL				P	Plagioclase	60/100	2.027	.254	31	88.1	.6
	1605-KF				P	K-feldspar	28/60	.481	11.67	2	87.0	.3
113	1606	36°26′29″	118°43′12″	4,800	P	Biotite	10/16	.390	7.239	19	88.5	.6

TABLE 5.—*Potassium-argon analyses and location of sample localities*—Continued

Location No. (pl. 1)	KA No.	Latitude (N.)	Longitude (W.)	Elevation (ft)	Picked (P) or unpicked (U)	Mineral	Size (standard mesh)	Weight (grams)	K (wt percent)	Ar_{at}^{40} (percent)	Age (10^6 yr)	$\delta_{(x-y)}$ (percent)
114	1607	36°27′48″	118°37′56″	7,000	P	Biotite	8/10	.436	7.536	26	88.9	.4
115	1608	36°27′22″	118°33′22″	12,340	P	do	16/28	.368	7.099	15	90.5	.1
	1608-R				P	do	16/28	.374	7.099	10	93.2	.1
116	1609	36°27′48″	118°32′46″	10,800	P	do	16/28	.334	7.290	13	87.4	.3
	1609-HBD				P	Hornblende	28/60	1.774	.974	17	93.0	.1
117	1610	36°27′37″	118°33′43″	11,600	P	Biotite	28/60	.291	6.773	19	88.3	.6
	1610-HBD				P	Hornblende	28/60	1.656	2.136	14	86.4	2.0
140	1621	35°12′43″	118°32′42″	2,700	P	Biotite	10/16	.323	7.272	19	81.2	.4
50	1624	38°04′18″	120°10′46″	------------	P	do	16/28	.300	7.727	6	138	.3
	1624-HBD				P	Hornblende	28/60	1.517	.727	11	136	.3
118	1626	36°26′35″	118°54′13″	------------	P	Biotite	8/10	.280	7.729	17	93.5	.5
	1626-HBD				P	Hornblende	28/60	2.148	.617	25	101	.6
87	1627	37°17′45″	119°31′52″	------------	P	Biotite	10/16	.206	7.694	8	97.7	.5
	1627-HBD				P	Hornblende	28/60	2.061	.628	30	100	.5
88	1628	37°19′05″	119°39′20″	------------	P	Biotite	16/28	.280	7.768	14	104	.4
	1628-HBD				P	Hornblende	16/28	2.051	.721	18	144	.2
119	1629	36°23′33″	118°57′55″	------------	P	Biotite	10/16	.305	7.564	8	103	.3
	1629-HBD				P	Hornblende	28/60	2.227	.456	26	105	.4
120	1630	36°17′45″	119°04′40″	------------	P	Biotite	28/60	.218	6.540	13	114	.2
	1630-HBD				P	Hornblende	28/60	.915	1.762	11	115	.7
142	1631	34°53′49″	118°55′01″	------------	P	Biotite	28/60	.278	7.349	21	86.1	.1
89	1632	37°58′45″	120°20′03″	------------	P	do	16/28	.261	7.438	10	152	.1
	1632-HBD				P	Hornblende	16/28	1.773	.955	26	162	.1
61	1633	38°25′00″	120°27′01″	------------	P	Biotite	16/28	.210	7.805	16	89.1	.0
	1633-HBD				P	Hornblende	16/28	1.893	.839	17	120	.0
90	1634	37°59′29″	120°16′37″	------------	P	Biotite	16/28	.244	7.763	5	144	.3
	1634-HBD				P	Hornblende	28/60	2.032	1.020	10	156	.9
51	1635	38°18′02″	120°16′38″	------------	P	Biotite	16/28	.261	7.812	20	125	.1
	1635-HBD				P	Hornblende	28/100	2.118	1.368	4	148	.1
52	1636	38°23′16″	120°11′01″	------------	P	Biotite	28/60	.204	7.535	11	96.0	.6
	1662-HBD	38°23′16″	120°11′01″	------------	P	Hornblende	28/60	2.076	.956	19	95.8	.4
91	1663-HBD	37°40′43″	119°45′47″	------------	P	do	16/28	1.171	1.004	11	101	.5
53	1664	38°13′01″	120°22′13″	------------	P	Biotite	16/28	.311	7.315	9	145	.6
	1664-HBD				P	Hornblende	28/60	1.269	.713	11	148	.6
92	1665-HBD	37°33′07″	119°40′53″	------------	P	do	28/60	2.114	.783	9	108	.4
93	1666	37°06′25″	119°44′36″	------------	P	Biotite	28/60	.364	7.709	5	107	.5
141	1667	35°01′35″	118°20′50″	------------	P	do	28/60	.339	7.207	13	80.4	.1
	1667-HBD				P	Hornblende	28/60	1.891	.936	17	81.4	.0
143	1668-HBD	34°39′34″	118°27′38″	------------	P	do	16/28	2.511	1.075	16	70.6	.5
144	1670-HBD	34°46′57″	119°03′32″	------------	P	do	28/60	2.412	1.213	5	69.7	.3
145	1671-HBD	34°29′19″	117°52′01″	3,300	P	do	10/16	2.015	.834	10	76.9	.1
146	1672	34°50′35″	119°21′06″	3,950	P	Biotite	28/60	.390	7.646	14	67.2	.0
	1672-HBD				P	Hornblende	28/60	2.272	1.069	11	69.5	.5
147	1673	34°49′28″	118°59′27″	5,450	P	Biotite	28/60	.414	7.393	5	76.9	.3
148	1674	34°27′55″	117°51′41″	3,500	P	do	16/28	.336	7.329	13	68.1	.1
	1674-HBD				P	Hornblende	16/28	2.193	1.028	29	73.1	.1
149	1675	34°20′51″	117°55′15″	6,810	P	Biotite	16/28	.337	7.500	13	64.7	.1
150	1676	34°41′56″	118°56′00″	3,800	P	do	28/60	.327	7.485	5	66.1	.7
151	1677	34°09′	116°58′	5,800	P	do	16/28	.314	7.574	5	69.7	.5
	1677-HBD				P	Hornblende	16/28	3.014	.866	9	72.6	.2
54	1678	38°47′02″	120°12′53″	5,360	P	Biotite	16/28	.331	7.467	13	92.8	.1
	1678-HBD				P	Hornblende	16/28	2.414	.668	9	97.6	.6
55	1679	38°48′20″	120°07′18″	6,310	P	Biotite	16/28	.338	7.515	6	93.7	.1
152	1680	34°15′47″	117°39′07″	7,220	P	do	28/60	.341	6.578	9	61.0	.6
	1680-HBD				P	Hornblende	28/60	2.135	1.057	42	71.5	.7
153	1682-HBD	34°52′54″	118°54′04″	3,150	P	do	16/28	2.179	.324	43	77.4	.2
56	1683	38°45′50″	120°19′38″	3,880	P	Biotite	10/16	.318	7.587	3	102	.8
	1683-HBD				P	Hornblende	10/16	2.525	.597	8	100	.2
154	1696	34°18′42″	118°08′15″	2,930	P	Biotite	28/60	.340	7.550	22	65.8	.6
	1696-HBD				P	Hornblende	28/60	1.683	.864	10	70.0	.7
57	1697	38°27′05″	119°27′29″	6,020	P	Biotite	16/28	.295	7.286	3	119	.7
58	1698	38°46′15″	120°23′01″	3,500	P	do	28/60	.293	7.538	6	108	.1
	1698-HBD				P	Hornblende	28/60	1.581	.775	6	140	.7
59	1699	38°46′23″	120°25′45″	3,400	P	Biotite	28/60	.365	7.875	16	117	.0
	1699-HBD				P	Hornblende	28/60	1.665	.713	4	140	.4
60	1700-HBD	38°46′17″	120°29′34″	3,320	P	do	16/28	2.522	.468	28	138	.2
18	1701	39°22′30″	121°05′	1,500	P	Biotite	16/28	.298	7.838	4	143	.2
	1701-HBD				P	Hornblende	16/28	2.245	.576	25	146	.2
19	1702	39°37′00″	129°27′06″	5,760	P	Biotite	28/60	.303	7.153	3	153	.1
	1702-HBD				P	Hornblende	28/60	2.097	.773	5	150	.4
209	DKA 1028	37°57′10″	119°14′06″	------------	U	Biotite	60/80	.297	7.495	8	83.7	----------
210	DKA 1029	37°57′10″	119°14′06″	------------	U	do	80/100	.222	7.412	10	84.8	----------
	MKA 409	37°57′10″	119°14′06″	------------	U	Hornblende	100/150	1.501	.777	29	94.8	----------
211	MKA 41	37°55′50″	119°14′30″	------------	U	Biotite	80/100	.698	6.050	11	93.9	----------
212	DKA 1031	37°57′11″	119°14′06″	------------	U	do	80/100	.241	7.528	6	83.2	----------
	DKA 1032	37°57′11″	119°14′06″	------------	U	Hornblende	100/150	1.478	.653	22	92.8	----------
213	DKA 1030	37°57′40″	119°12′30″	------------	U	Biotite	80/100	.301	7.669	10	99.0	----------
	MKA 410	37°57′40″	119°12′30″	------------	U	Hornblende	100/150	2.696	.446	22	206.0	----------
214	BKA 558	37°58′00″	119°12′22″	------------	U	Biotite	60/80	1.061	6.250	33	82.0	----------
215	MKA 42	37°56′05″	119°10′00″	------------	U	do	40/60	1.014	6.960	9	89.6	----------
216	BKA 488	37°51′30″	119°04′52″	------------	U	do	80/100	1.109	7.470	12	87.7	----------
	61-192	37°51′30″	119°04′52″	------------	U	Hornblende	100/150	.993	.377	15	85.5	----------
217	BKA 487	37°46′20″	119°04′58″	------------	U	Biotite	40/60	.671	7.450	21	87.9	----------
	MKA 458	37°46′20″	119°04′58″	------------	U	Hornblende	100/115	1.077	.643	43	97.1	----------
218	BKA 556	37°46′50″	119°13′55″	------------	U	Biotite	60/80	1.544	6.820	12	82.4	----------
219	BKA 557	37°45′05″	119°10′00″	------------	U	do	60/80	.840	6.240	22	69.0	----------
220	61-041	37°06′25″	119°44′36″	------------	U	Muscovite	35/80	.580	8.580	7	109.9	----------
	61-042	37°06′25″	119°44′36″	------------	U	Biotite	35/60	.442	7.530	13	110.0	----------
221	61-001	37°15′50″	118°45′48″	------------	U	do	60/80	.559	7.340	9	80.3	----------
	61-020	37°15′50″	118°45′48″	------------	U	Hornblende	80/100	1.490	.607	12	83.3	----------
222	MKA 51	36°33′40″	117°54′20″	------------	U	Biotite	60/80	.311	3.400	21	134.0	----------
201	61-047	36°55′10″	118°08′09″	------------	U	Hornblende	100/115	.621	.599	12	155.5	----------
203	61-043	36°49′48″	118°02′05″	------------	U	do	80/100	.945	.569	15	163.1	----------
223	61-045	36°44′58″	118°02′10″	------------	U	do	100/115	.623	.487	17	177.6	----------
224	61-044	36°39′47″	117°59′05″	------------	U	do	100/115	.437	1.050	15	162.6	----------
225	61-005	37°56′20″	118°20′10″	------------	U	Biotite	80/100	.859	6.960	6	156.7	----------

TABLE 5.—*Potassium-argon analyses and location of sample localities*—Continued

Location No. (pl. 1)	KA No.	Latitude (N.)	Longitude (W.)	Elevation (ft)	Picked (P) or unpicked (U)	Mineral	Size (standard mesh)	Weight (grams)	K (wt percent)	Ar_{at}^{40} (percent)	Age (10^6 yr)	$\delta_{(x-y)}$ (percent)
226	61-019	37°47′05″	118°28′30″	------------	U	Biotite	60/80	.599	7.060	9	149.2	---------
	61-025	37°47′05″	118°28′30″	------------	U	Hornblende	100/115	1.339	.744	6	157.5	---------
227	51-166	37°47′05″	118°28′30″	------------	U	Biotite	60/80	.504	7.010	9	153.5	---------
228	61-003	37°55′50″	118°49′50″	------------	U	do	60/80	.886	6.470	36	139.4	---------
229	61-017	37°56′59″	118°53′48″	------------	U	Hornblende	100/115	1.943	.896	6	195.0	---------
230	61-008	37°53′10″	118°37′30″	------------	U	Biotite	60/80	.355	6.830	4	210.2	---------
	61-026	37°53′10″	118°37′30″	------------	U	Hornblende	100/115	2.019	.896	5	206.2	---------
231	61-190	38°56′40″	118°50′10″	------------	U	do	100/115	.976	.735	9	140.4	---------
232	61-191	38°43′12″	118°26′45″	------------	U	do	100/115	1.663	.585	20	89.1	---------
233	61-007	38°39′30″	118°31′05″	------------	U	Biotite	60/80	.569	5.880	8	93.8	---------
	61-018	38°39′30″	118°31′05″	------------	U	Hornblende	100/115	1.001	.512	42	90.2	---------
234	61-022	38°35′15″	118°04″50′	------------	U	do	100/115	1.363	.551	62	84.3	---------
235	71-002	38°26′17″	118°12′42″	------------	U	Biotite	60/80	.195	6.170	15	91.9	---------
236	71-006	38°26′17″	118°47′02″	------------	U	do	60/80	.198	6.860	15	75.4	---------
237	61-194	38°19′07″	118°37′30″	------------	U	Hornblende	100/115	1.002	.411	27	75.3	---------
238	71-022	38°16′20″	118°28′50″	------------	U	Biotite	60/80	.202	8.150	21	86.1	---------
	61-196	38°16′20″	118′28°50″	------------	U	Hornblende	100/150	1.005	.466	32	100.5	---------
239	61-188	38°11′50″	118°31′15″	------------	U	do	100/115	1.000	.560	27	101.9	---------
240	71-079	34°02′10″	117°33′26″	------------	U	Biotite	60/80	.203	7.420	31	94.2	---------
	71-073	34°02′10″	117°33′26″	------------	U	Hornblende	100/150	.998	1.190	52	95.0	---------
241	71-075	33°55′20″	117°19′06″	------------	U	Biotite	60/80	.194	7.880	5	94.1	---------
	71-061	33°55′20″	117°19′06″	------------	U	Hornblende	100/115	1.003	.593	40	94.7	---------
242	71-063	33°54′40″	117°15′12″	------------	U	do	100/115	1.002	.688	11	96.4	---------
243	71-081	33°36′12″	117°12′30″	------------	U	Biotite	60/80	.197	7.780	9	98.4	---------
	71-071	33°36′12″	117°12′30″	------------	U	Hornblende	100/115	.993	.838	10	101.9	---------
244	71-077	33°31′02″	116°42′10″	------------	U	Biotite	60/80	.204	7.820	13	85.9	---------
	71-065	33°31′02″	116°42′10″	------------	U	Hornblende	100/150	.987	.889	48	87.7	---------
245	71-083	33°07′15″	117°08′22″	------------	U	Biotite	60/80	.171	7.550	33	91.1	---------
	71-067	33°07′15″	117°08′22″	------------	U	Hornblende	100/115	.994	.549	19	101.1	---------
246	71-069	33°05′40″	116°56′40″	------------	U	do	100/115	1.003	.671	56	104.9	---------
247	61-119	36°15′10″	121°32′30″	------------	U	do	100/115	1.075	.548	32	75.8	---------
248	61-117	36°15′10″	121°32′30″	------------	U	do	100/115	1.120	.880	30	77.2	---------
249	MKA-399	38°18′40″	123°04′15″	------------	U	do	100/115	2.152	.830	13	92.0	---------

Ages of South American granitic rocks not shown on plates 1 and 2

KA No.	Latitude (N. and S.)	Longitude (W.)	Elevation (ft)	Picked (P) or unpicked (U)	Mineral	Size (standard mesh)	Weight (grams)	K (wt percent)	Ar_{at}^{40} (percent)	Age (10^6 yr)
591	16°30′S	67°50′	------------	U	Biotite			7.24	10	199.0
620	16°18′S	67°52′	------------	U	Muscovite			8.56	2	183.0
634	10°54′S	76°02′	------------	U	do			10.85	5	195.0
1466	17°43′S	70°03′	------------	U	do			7.66	2	187.0
1158	16°10′S	73°09′	------------	U	Biotite			6.72	4	204.0
1159	13°52′S	70°22′	------------	U	do			6.51	3	180.0
1145	14°06′S	70°02′	------------	U	do			7.08	6	207.0
1155	13°29′S	70°42′	------------	U	do			6.43	5	213.0
1454	16°07′S	68°07′		U	do			7.66	3	211.0
1374	15°08′N	89°32′	------------	U	do			5.24	7	178.0
615	15°55′S	68°28′	------------	U	do			6.42	9	180.0

TABLE 6.—*Rock name and description of sample locality*

[Latitudes and longitudes given in table 5]

KA No. (unless otherwise indicated)	*Rock name*	*Locality*
477	Trondhjemite of Caribou Mountain (Davis, 1961).	Coffee Creek quadrangle, California.
579	Quartz monzonite of Beer Creek (McKee and Nelson, 1967).	Behind large garage and storage shed immediately behind (east of) Deep Springs School, Soldier Pass quadrangle, California–Nevada.
668	Unnamed (Christensen, 1959).	Along trail in pass between Columbine Lake and Lost Canyon, Kaweah quadrangle, California.
804	Papoose Flat pluton	Papoose Flat, Inyo Mountain, Waucoba Mountain quadrangle, California.
820	Isabella Granodiorite of Miller (1931).	Survey Point 3135T, near Kern River, northwest of Yellowjacket, Kernville quadrangle, California.
822	Isabella Granodiorite ("foliated") of Miller (1931).	SE¼SW¼ sec. 11, R. 33 E., T. 25 S., about ½ mile east of eastern branch of Kern Canyon fault, Isabella quadrangle, California.
828	Trondhjemite of Horseshoe Lake (Davis, 1961).	From ridge west of Forest Peak, Minersville quadrangle, California.
840	Granite of Sylvania Mountain.	Highest point on Sylvania Mountain, 7,998 ft, Magruder Mountain quadrangle, Nevada–California.
842	Hornblende diorite (Hay, 1963).	Western side of Gold Hill, northern part of lot 37, Cholame Ranch quadrangle, California.
902	Quartz monzonite of Beer Creek (McKee and Nelson, 1967).	1 mile north of Sugarloaf Mountain, Soldier Pass quadrangle, California–Nevada.
955	Unnamed (Romey, 1962).	SW¼ sec. 35, T. 41 N., R. 10 W., Etna quadrangle, California.
956	do	West end of Statue Lake, Etna quadrangle, California.
957	Quartz diorite of Deadman Peak (Holdaway, 1963).	6.36 miles S. 17° E. of northwest corner of Coffee Creek quadrangle, California.
1432	Elephant Butte pluton (Gromme, 1963).	1,000 ft south of Rock Creek in canyon of North Fork of Feather River, Pulga quadrangle, California.
1433	do	Do.
1436	Bucks pluton (Gromme, 1963).	½ mile north of Workman's Bar in canyon of North Fork of Feather River, Pulga quadrangle, California.
1437	do	Do.
1438	Merrimac pluton (Gromme, 1963).	1 mile southwest of Merrimac near Coon Creek, Pulga quadrangle, California.
1439	do	Do.
1440	Cresta pluton (Gromme, 1963).	¼ mile north of Cresta powerhouse, in canyon of North Fork of Feather River, Pulga quadrangle, Califorina.
1441	do	Do.
1442	Bucks pluton (Gromme, 1963).	At Workman's Bar, in canyon of North Fork of Feather River, Pulga quadrangle, California.
1449	do	Do.
1501	Unnamed	Deans Ridge, Eagle Lake, at 5,600 ft on dirt road, Fredonyer Peak quadrangle, California.
1502	do	Northeast slope of Deans Ridge, at 5,350 ft on road, Fredonyer Peak quadrangle, California.
1503	do	On Janesville Grade, at ridge line of secondary ridge immediately east of main volcanic-capped ridge, Susanville quadrangle, California.
1504	do	Head of Janesville Grade, at intersection of Thompson Creek Road and road to Thompson Peak lookout, Kettle Rock quadrangle, California.
1506	do	¼ mile west of Forest Service Road 27N03, on Road 27N12, Plumas National Forest, Milford quadrangle, California.

TABLE 6.—*Rock name and description of sample locality*—Con.

KA No. (unless otherwise indicated)	*Rock name*	*Locality*
1508	Unnamed	Beckwourth Pass, from Western Pacific Railroad tunnel, Chilcoot quadrangle, California.
1509	do	On Forest Service road 27N02 at road intersection in SW¼ sec. 3, T. 23 N., R. 14 E., Portola quadrangle, California.
1510	do	Yuba Pass, California State Highway 49, ½ mile southwest of pass on dirt road, Sierraville quadrangle, California.
1511	do	1.1 miles east of Yuba Pass on California State Highway 49, Sierraville quadrangle, California.
1512	do	BM 6680 on U.S. Highway 40, just east of Donner Summit, Donner Pass quadrangle, California.
1514	do	Base of west wall of Angora Peak, perpendicular to stream at first trail crossing on Lake of Woods trail, Fallen Leaf Lake quadrangle, California.
1516	do	Daggett Pass, Nevada State Highway 19, Freel Peak quadrangle, California–Nevada.
1517	do	At Daggett Creek on Nevada State Highway 19, Freel Peak quadrangle, California–Nevada.
1518	do	At 7,500 ft in Horsethief Canyon, Freel Peak quadrangle, California–Nevada.
1519	do	On west side of Carson Pass at 7,250 ft on California State Highway 88, Silver Lake quadrangle, California.
1520	do	East of Carson Spur at 7,720 ft on California State Highway 88, Silver Lake quadrangle, California.
1521	Carson Pass Tonalite of Parker (1961).	Summit, Carson pass on California Highway 88, Markleeville quadrangle, California.
1523	Stanislaus Meadow Adamellite of Parker (1961).	At 7,500 ft on California State Highway 4, east of Lake Alpine, Dardanelles Cone quadrangle, California.
1524	Unnamed	At 7,600 ft on California State Highway 4, east of Ebbetts Pass, just east of Silver Creek, Markleeville quadrangle, California.
1525	Half Dome Quartz Monzonite (Calkins, 1930).	May Lake trailhead, Hetch Hetchy quadrangle, California.
1526	Transition zone between Half Dome Quartz Monzonite and Cathedral Peak Granite (Calkins, 1930).	At 8,800 ft on southeast flank of Polly Dome, Tuolumne Meadows quadrangle, California.
1527	Cathedral Peak Granite (Calkins, 1930).	At 8,800 ft on east side of Polly Dome, Tuolumne Meadows quadrangle, California.
1528	do	At 8,800 ft on north nose of Fairview Dome, Tuolumne Meadows quadrangle, California.
1530	do	At 9,000 ft on Echo Creek, Tuolumne Meadows quadrangle, California.
1531	do	At 9,000 ft on shore of Babcock Lake, Tuolumne Meadows quadrangle, California.
1532	Half Dome Quartz Monzonite (Calkins, 1930).	At 8,800 ft on John Muir Trail in Lyell Fork Canyon, Tuolumne Meadows quadrangle, California.
1533	Cathedral Peak Granite (Calkins, 1930).	At 8,800 ft on John Muir Trail in Lyell Fork Canyon, Tuolumne Meadows quadrangle, California.
1534	Quartz monzonite of Topaz Lake (Cathedral Peak type) (Curtis, 1951).	At 6,640 ft on Wolf Creek, Topaz Lake quadrangle, California.
1535	Quartz monzonite of Topaz Lake (Cathedral Peak type) (Slemmons, 1953).	Head of Clark Fork of Stanislaus River at 10,200 ft, Sonora Pass quadrangle, California.
1536	do	At 7,450 ft on west side of The Iceberg, Sonora Pass quadrangle, California.

TABLE 6.—*Rock name and description of sample locality*—Con.

KA No. (unless otherwise indicated)	*Rock name*	*Locality*
1537	Quartz monzonite of Topaz Lake (Cathedral Peak type) (Slemmons, 1953).	At BM 5831 on California State Highway 108, Dardanelles Cone quadrangle, California.
1538	Granodiorite west of quartz monzonite of Topaz Lake (Slemmons, 1953).	At Clark Fork Bridge, Dardanelles Cone quadrangle, California.
1539	do	At Niagara Creek on California State Highway 108, Dardanelles Cone quadrangle, California.
1540	Unnamed	½ mile north of Cascade Creek at 6,080 ft on California State Highway 108, Dardanelles Cone quadrangle, California.
1541	do	On California State Highway 108 at roadcut west of Strawberry Resort at 5,250 ft, Long Barn quadrangle, California.
1542	Granodiorite west of quartz monzonite of Topaz Lake (Slemmons, 1953).	At 7,650 ft between Fence and Cloudburst Creeks, Dardanelles Cone quadrangle, California.
1543	Quartz monzonite of Topaz Lake (Cathedral Peak type) (Slemmons, 1953).	At 7,600 ft on west side of Cloudburst Creek, Dardanelles Cone quadrangle, California.
1545	do	On California State Highway 108 at bridge crossing of Kennedy Creek, Sonora Pass quadrangle, California.
1546	do	At 7,500 ft in Woods Gulch, Dardanelles Cone quadrangle, California.
1547	do	At 7,400 ft in Woods Gulch, Dardanelles Cone quadrangle, California.
1548	do	At 7,600 ft along East Fork of Carson River, Sonora Pass quadrangle, California.
1549	do	At 7,500 ft on Boulder Creek, Sonora Pass quadrangle, California.
1550	do	At 10,040 ft at head of Silver Creek, Sonora Pass quadrangle, California.
1551	Quartz monzonite of Mono Recesses (Cathedral Peak type) (Sherlock and Hamilton, 1958).	At 11,500 ft on ridge west of Lower Hopkins Lake, Mount Abbot quadrangle, California.
1552	do	At 9,000 ft on Mono Creek, Mount Abbot quadrangle, California.
1553	do	At 11,500 ft on west side of Mono Pass, Mount Abbot quadrangle, California.
1554	Quartz monzonite of Lagille Peak (Cathedral Peak type).	At 11,500 ft on north shoulder of Shakespeare Peak, Mount Goddard quadrangle, California.
1555	do	At 8,080 ft on Middle Fork of Kings River above junction with Palisade Creek, Mount Goddard quadrangle, California.
1556	Cathedral Peak type	At 11,500 ft along trail on west side Kearsarge Pass, Mount Pinchot quadrangle, California.
1559	Quartz monzonite of Mono Recesses (Cathedral Peak type).	Top of hill 9247, north-northwest of Devil's Postpile National Monument, Devil's Postpile quadrangle, California.
1560	do	At 9,000 ft in hill 9247, Devil's Postpile quadrangle, California.
1561	do	At 11,500 ft in Granite Park, Mount Abbott quadrangle, California.
1562	Isabella Granodiorite and its facies (Miller, 1931; Miller and Webb, 1940).	At 2,800 ft in SW¼ sec. 32, T. 24 S., R. 33 E., Kernville 30 minute quadrangle, California.
1563	do	At 4,000 ft in center sec. 35, T. 22 S., R. 32 E., Kernville 30 minute quadrangle, California.
1564	do	At 6,200 ft on road, south side of Horse Canyon, Camp Nelson quadrangle, California.
1565	Unnamed	1.4 miles south of road crossing of Boulder Creek on California State Highway 190, on west-facing side of ridge, Camp Nelson quadrangle, California.

TABLE 6.—*Rock name and description of sample locality*—Con.

KA No. (unless otherwise indicated)	Rock name	Locality
1566	Unnamed	At McIntyre Creek on California State Highway 190, Camp Nelson quadrangle, California.
1568	do	On California State Highway 190, just west of Coffee Creek Picnic Ground, Camp Nelson quadrangle, California.
1569	do	In most westerly ¼ mile of granite outcrops west-northwest of Woody on Woody-Delano Road, 6.4 miles west of Woody, Woody quadrangle, California.
1570	do	1.2 miles northeast of Woody on Woody-Greenhorn Summit road, Woody quadrangle, California.
1571	do	1.4 miles west of Lynns Valley on Woody-Greenhorn Summit road, Woody quadrangle, California.
1572	do	3.65 miles east of Glennville on Woody-Greenhorn Summit road, Tobias Peak 30 minute quadrangle, California.
1573	do	3.50 miles east of west boundary of Sequoia National Forest, just west of Cedar Creek on highway, Tobias Peak quadrangle, California.
1574	do	1.25 miles east of Greenhorn Summit at 5,780 ft on highway, Tobias Peak 30 minute quadrangle, California.
1575	do	At 3,750 ft on highway 5.6 miles east of Greenhorn Summit, Kernville 30 minute quadrangle, California.
1576	do	French Gulch, at Kern County Camp No. 3 on Kernville-Isabella road, Isabella quadrangle, California.
1577	do	On California State Highway 178, 3.0 miles east of intersection with Kernville-Isabella road, Isabella quadrangle, California.
1578	Unnamed	1.2 miles west of Weldon on California State Highway 178, Isabella quadrangle, California.
1579	do	1.2 miles east of Onyx on California State Highway 178, Onyx quadrangle, California.
1580	do	At 2,900 ft on California State Highway 178, on west end of ridge across creek from Bloomfield Ranch, Onyx quadrangle, California.
1581	do	At 3,450 ft on California State Highway 178, approximately 0.55 miles west of intersection of Canebrake and Spanish Needle Creeks, Lamont Peak quadrangle, California.
1582	do	At 4,410 ft on California State Highway 178, just west of intersection of Canebrake and Three Pines Canyon Creeks, Onyx quadrangle, California.
1583	Cathedral Peak type	Alabama Hills, on road to Whitney Portal, Lone Pine quadrangle. California.
1584	Whitney pluton	At Whitney Portal, 8,480 ft, Lone Pine quadrangle, California.
1585	do	At 9,500 ft on Olancha Peak, Olancha quadrangle, California.
1586	do	At 9,680 ft on Golden Trout Creek, Kern Peak quadrangle, California.
1587	do	At 9,280 ft on Wallace Creek Trail, Mount Whitney quadrangle, California.
1588	do	At 11,530 ft on west side of Trailcrest along trail, Mount Whitney quadrangle. California.
1589	do	At 11,500 ft along Tyndall Creek, Mount Whitney quadrangle, California.
1590	do	At Trailcrest, 13,777 ft, Mount Whitney quadrangle, California.

TABLE 6.—*Rock name and description of sample locality*—Con.

KA No. (unless otherwise indicated)	*Rock name*	*Locality*
1591	Unnamed	At 11,600 ft on east side of Trailcrest along trail, Mount Whitney quadrangle, California.
1592	do	At 7,680 ft on Whitney Portal Road, Lone Pine quadrangle, California.
1593	Cathedral Peak Granite.	40 ft below summit of Cathedral Peak, Tuolumne Meadows quadrangle, California.
1594	do	At 8,700 ft on east flank of Lembert Dome, Tuolumne Meadows quadrangle, California.
1595	do	At 11,000 ft on high point of ridge west of Little Slide C Canyon, Matterhorn Peak quadrangle, California.
1596	do	At 9,200 ft west-northwest from KA 1595 on small tributary stream entering Robinson Creek from southeast, Matterhorn Peak quadrangle, California.
1597	do	At 7,950 ft on Twin Lake–Barney Lake trail, Matterhorn Peak quadrangle, California.
1598	do	At 7,300 ft on Barney Lake trail, Matterhorn Peak quadrangle, California.
1599	do	At 9,000 ft on Kirkwood Creek, Tower Peak quadrangle California.
1600	Quartz monzonite of Lagille Peake (Cathedral Peak type).	At 11,500 ft on west side of Hermit Ridge, McGee Lakes basin, Mount Goddard quadrangle, California.
1601	Lamarck Granodiorite.	At 12,880 ft from Lamarck Col, Mount Goddard quadrangle, California.
1602	Unnamed	At 2,400 ft on Mineral King road, Mineral King quadrangle, California.
1603	do	At 3,050 ft on Mineral King road, Mineral King quadrangle, California.
1604	do	At 3,900 ft on Mineral King road, Mineral King quadrangle, California.
1605	Unnamed	At 4,050 ft on Mineral King road, Mineral King quadrangle, California.
1606	do	At 4,800 ft on Mineral King road, Mineral King quadrangle, California.
1607	do	At 7,000 ft on Mineral King road, 1 mile east of Silver City, Mineral King quadrangle, California.
1608	do	At top of Sawtooth Peak, 12,340 ft, Kaweah quadrangle, California.
1609	do	At 10,800 ft, head of Lost Canyon, east of Columbine Lake (virtually same locality as KA 1608), Kaweah quadrangle, California.
1610	do	At 11,600 ft in Sawtooth Pass, Kaweah quadrangle, California.
1621	do	8.2 miles west of Tehachapi Railroad Station on California State Highway 58 (U.S. Highway 466) at 2,700 ft, Tehachapi quadrangle, California.
1624	do	1.0 mile east of Mi-wuk Village on California State Highway 108, Long Barn quadrangle, California.
1626	do	At east end of business district of Three Rivers on California State Highway 198.
1627	do	At southeast end of Bass Lake from borrow pit for dam, Bass Lake quadrangle, California.
1628	do	0.8 mile west of west end of Oakhurst bridge on California State Highway 41, Bass Lake quadrangle, California.
1629	do	1.05 miles west of Horse Creek Road turnoff, 4.75 miles east of Woodlake turnoff on California State Highway 198.

TABLE 6.—*Rock name and description of sample locality*—Con.

KA No. (unless otherwise indicated)	*Rock name*	*Locality*
1630	Unnamed	0.8 mile northeast of hill 1560, approximately 12.5 miles S. 81° E. of Visalia, Visalia quadrangle, California.
1631	do	At 2,600 ft on Grapevine, U.S. Highway 99.
1632	do	2.95 miles east of Sonora city limits, 1.0 mile east of Tuolumne City turnoff, on California State Highway 108, Sonora quadrangle California.
1633	do	At Big Meadows Campground on California State Highway 4, Big Meadow quadrangle, California.
1634	do	0.65 mile west of Soulsbyville turnoff, 2.6 miles east of Standard turnoff, on California State Highway 108, Sonora quadrangle, California.
1635	do	0.1 mile west of Dorrington on California State Highway 4 at 4,800 ft, Blue Mount quadrangle, California.
1636	do	0.5 mile west of Poison Spring at 6,560 ft on California State Highway 4, Big Meadow quadrangle, California.
1663	Granodiorite of The Gateway (Calkins, 1930).	At west park boundary of Yosemite National Park on California State Highway 140.
1664	Unnamed	0.8 mile east of Avery at 3,500 ft on California State Highway 4, Columbia quadrangle, California.
1665	do	1.9 miles northwest of Wawona on California State Highway 41 at approximately 4,200 ft, Yosemite National Park.
1666	do	5.2 miles east of Road 208, 7.3 miles east of California State Highway 145, on California State Highway 41, at 1,150 ft.
1678	Unnamed	1.5 miles west of Pyramid Campground on U.S. Highway 50, Fallen Leaf Lake quadrangle, California.
1679	do	Approximately ½ mile east of hairpin turn, at 90° turn, west of Camp Sacramento on U.S. Highway 50, Fallen Leaf Lake quadrangle, California.
1683	do	0.8 mile west of Silver Fork at 3,880 ft on U.S. Highway 50, Robbs Peak quadrangle, California.
1697	do	At 6,020 ft on west side of U.S. Highway 395 along West Walker River at north end of Shingle Mill Flat.
1698	do	4.5 miles west of Silver Fork at 3,500 ft on U.S. Highway 50, Robbs Peak quadrangle, California.
1699	do	1.6 miles west of Whitehall on U.S. Highway 50, Robbs Peak quadrangle, California.
1700	do	4.8 miles west of Whitehall, 0.5 mile east of Bridalveil picnic area, on U.S. Highway 50, Robbs Peak quadrangle, California.
1701	do	Where California State Highway 49 crosses Middle Fork Yuba River, Camptonville quadrangle, California.
1702	do	1.3 miles west of Chapman Creek Campground on California State Highway 49, Sierra City quadrangle, California.
DKA 1028	Granodiorite of Mono Dome (Kistler, 1966a).	California State Highway 120, 1 mile north of Ellery Lake, Mono Craters quadrangle, California.
DKA 1029	do	California State Highway 120, 1 mile north of Ellery Lake, Mono Craters quadrangle, California.

TABLE 6.—*Rock name and description of sample locality*—Con.

KA No. (unless otherwise indicated)	*Rock name*	*Locality*
MKA 409	Granodiorite of Mono Dome (Kistler, 1966a).	California State Highway 120, 1 mile north of Ellery Lake, Mono Craters quadrangle, California.
MKA 41	Quartz monzonite of Ellery Lake (Kistler 1966a).	Hill 11582 on Dana Plateau, Mono Craters quadrangle, California.
DKA 1031	Granodiorite of Mono Dome (Kistler, 1966a).	California State Highway 120, 1.2 miles north of Ellery Lake, Mono Craters quadrangle, California.
DKA 1032	do	California State Highway 120, 1.2 miles north of Ellery Lake, Mono Craters quadrangle, California.
DKA 1030	do	Elevation 11,100 ft, 1.2 miles southeast of Lee Vining Peak, Mono Craters quadrangle, California.
MKA 410	do	Elevation 11,100 ft, 1.2 miles southeast of Lee Vining Peak, Mono Craters quadrangle, California.
BKA 558	do	BM 8615, California State Highway 120, Mono Craters quadrangle, California.
MKA 42	Wheeler Crest Quartz Monzonite (Kistler, 1966a).	Hill 9962, 2 miles south of Mono Dome, Mono Craters quadrangle, California.
BKA 488	Quartz monzonite of Aeolian Buttes (Kistler, 1966a).	Hill 7451, Aeolian Buttes, Mono Craters quadrangle, California.
61–192	do	Hill 7451, Aeolian Buttes, Mono Craters quadrangle, California.
BKA 487	Wheeler Crest Quartz Monzonite (Kistler, 1966a).	Roadcut, just northeast, of town of June Lake, Mono Craters quadrangle, California.
MKA 458	do	Roadcut, just northeast of town of June Lake, Mono Craters quadrangle, California.
BKA 556	Granodiorite of Kuna Crest (Kistler, 1966a).	Elevation 11,600 ft, 0.25 mile north of Donohue Peak, Mono Craters quadrangle, California.
BKA 557	Granodiorite of Rush Creek (Kistler, 1966a).	0.2 mile west of Billy Lake, Mono Craters quadrangle, California.
61–041	Unnamed	Quarry, 1 mile south of Knowles, Raymond quadrangle, California.
61–042	Unnamed	Quarry, 1 mile south of Knowles, Ráymond quadrangle, California.
61–001	Tungsten Hills Quartz Monzonite (Bateman, 1961).	Elevation 10,000 ft, North Fork, Piute Creek, Mount Abbot quadrangle, California.
61–020	do	Elevation 10,000 ft, North Fork, Piute Creek, Mount Abbot quadrangle, California.
MKA 51	Unnamed	Burgess mine, New York Butte quadrangle, California.
61–047	Santa Rita Flat pluton of the Tinemaha Granodiorite (Ross, 1965).	Independence quadrangle, California.
61–043	Quartz monzonite of Piute Monument (Ross, 1965).	Independence quadrangle, California.
61–045	Tinemaha Granodiorite (Ross, 1965).	Independence quadrangle, California.
61–044	Pat Keys pluton (Ross, 1965).	Waucoba Mountain quadrangle, California.
61–019	Unnamed	Comanche Gulch, Blind Spring Hill, Benton quadrangle, California.
61–025	do	Comanche Gulch, Blind Spring Hill, Benton quadrangle, California.
61–166	do	Comanche Gulch, Blind Spring Hill, Benton quadrangle, California.
61–003	do	3 miles south of Cowtrack Mountain, Cowtrack Mountain quadrangle, California.
61–017	do	2 miles southwest of Cowtrack Mountain, Cowtrack Mountain quadrangle, California.
61–008	do	California State Highway 120, 1.5 miles south of River Spring Lakes, Glass Mountain quadrangle, California.
61–026	do	California State Highway 120, 1.5 miles south of River Spring Lakes, Glass Mountain quadrangle, California.
61–190	do	2 miles west of Schurz, Nev., north end of Wassuk Range.
61–191	do	Valley between Gillis and Gabbs Valley Ranges, Nev., 1 mile east of Ryan Canyon Road.

TABLE 6.—*Rock name and description of sample locality*—Con.

KA No. (unless otherwise indicated)	*Rock name*	*Locality*
61–007	Unnamed	At crest of Gillis Range, Nev., on Ryan Canyon Road.
61–018	do	At crest of Gillis Range, Nev., on Ryan Canyon Road.
61–022	do	Just east of Nevada State Highway 23 in Gabbs Valley Range.
71–002	do	In Garfield Hills, due south of Luning, Nev.
71–006	do	On Bodie-Lucky Boy Road, due south of Cory Peak, Wassuk Range, Nev.
61–194	do	Mouth of Powell Canyon, Wassuk Range, Nev.
71–022	do	On road from Hawthorne, Nev., to Huntoon Valley, Nev., north side of Excelsior Mountains.
61–196	do	On road from Hawthorne, Nev., to Huntoon Valley, Nev., north side of Excelsior Mountains.
61–188	do	On road from Hawthorne, Nev., to Huntoon Valley, Nev., at north end of Huntoon Valley.
71–079	Granite of Rubidoux Mountain (Larsen, 1948).	Mount Rubidoux, Riverside West, 7.5-minute quadrangle, California.
71–073	do	Mount Rubidoux, Riverside West, 7.5-minute quadrangle, California.
71–083	San Marcos Gabbro (Larsen, 1948).	Twin Oaks Valley Road, quarry in Gopher Canyon, San Marcos, 7.5-minute quadrangle, California.
71–067	do	Twin Oaks Valley Road, quarry in Gopher Canyon, San Marcos 7.5-minute quadrangle, California.
71–069	Green Valley Tonalite.	California State Highway 78, 1 mile east of San Pasqual Battlefield State Historical Monument, San Pasqual 7.5-minute quadrangle, California.
61–119	Biotite hornblende gabbro (Compton, 1966).	Hornblendite in Arroyo Seco, ⅛ mile north-northwest of confluence with Santa Lucia Creek, Junipero Serra quadrangle, California.
61–117	Biotite hornblende gabbro (Compton, 1966).	Northwest end of main Junipero Serra Pluton, Junipero Serra quadrangle, California.
MKA 399	Granodiorite	Bodega Head, Sonoma County, Calif.
591	Unnamed	Mururata-Tasquesi, Bolivia.
71–075	Bonsall Tonalite (Larsen, 1948).	Val Verdi Tunnel, Cajalco Road, Steele Peak, 7.5-minute quadrangle, California.
71–061	do	Val Verdi Tunnel, Cajalco Road, Steele Peak, 7.5-minute quadrangle, California.
71–063	Lakeview Mountain Tonalite (Larsen, 1948).	Nuevo Road, 2 miles west of Nuevo, Perris 7.5-minute quadrangle, California.
71–081	Woodson Mountain Granodiorite (Larsen, 1948).	U.S. Highway 395, near intersection with road to Rainbow, Temecula 7.5-minute quadrangle, California.
71–071	do	U.S. Highway 395, near intersection with road to Rainbow, Temecula 7.5-minute quadrangle, California.
71–077	Sphene-rich tonalite	Near Tool Box Spring, Thomas Mountain, Idyllwild quadrangle, California.
71–065	do	Near Tool Box Spring, Thomas Mountain, Idyllwild quadrangle, California.
620	Muscovite from cassiterite vein.	Chojilla, Unduavi, Bolivia.
634	Granite	Carhuamayo, Peru.
1466	Gneiss	Cerro Machani, Peru.
1158	Small stock, intrudes Mitu Group of Middle to Late Permian age.	Ocona, Peru.
1159	Syenite, cuts Mitu Group.	Oscuyo-Ayapata, Peru.
1145	Cumbre de Achasiri granite (60 km × 15 km), intrudes Pennsylvanian and older rocks.	Cumbre de Achasiri-Coasa, Peru.
1155	Diorite	Cañon de Marcapata, Peru.
1454	Granite, intrudes Devonian sedimentary rocks.	H. Potosi batholith, Bolivia.
1374	Gneiss	Jones, Guatemala.
615	Sorata batholith	Candelaria, Cooco, Bolivia.

U.S. GOVERNMENT PRINTING OFFICE: 1969 O—359-835